High-Resolution Transmission Spectroscopy of Gas Giant Atmospheres

Prinoth, Bibiana

High-Resolution Transmission Spectroscopy of Gas Giant Atmospheres

BIBIANA PRINOTH
DIVISION OF ASTROPHYSICS | DEPARTMENT OF PHYSICS | LUND UNIVERSITY

High-Resolution Transmission Spectroscopy of Gas Giant Atmospheres

Bibiana Prinoth

Lund University

Thesis for the degree of Doctor of Philosophy

Thesis advisor: Dr. H. Jens Hoeijmakers
Co-advisors: Dr. Brian Thorsbro, Prof. Dr. David Hobbs
Faculty opponent: Prof. Dr. Neale Gibson

To be presented, with the permission of the Faculty of Science of Lund University, for public criticism in Rydbergsalen at the Division of Astrophysics, Department of Physics on Friday, 9th of May 2025 at 9:15.

Organization LUND UNIVERSITY Division of Astrophysics, Department of Physics, Box 118, SE-221 00, Lund, Sweden **Author(s)** BIBIANA PRINOTH	**Document name** DOCTORAL DISSERTATION **Date of issue** 2025-03-25 Sponsoring organization

Title and subtitle
High-resolution transmission spectroscopy of gas giant atmospheres

Abstract

The discovery of exoplanets has revealed an intriguing class of planets unlike anything in the Solar System: ultra-hot Jupiters. These gas giants share similarities with Jupiter in size and in their hydrogen- and helium-dominated atmospheres, yet their proximity to their host stars results in vastly different atmospheric conditions. Intense stellar radiation heats them to temperatures exceeding 2000 K, allowing metals such as iron and titanium to exist in the gas phase rather than condensing out. Among these species, titanium oxide (TiO) is of particular interest, as it has long been hypothesised to drive thermal inversions—temperature increases with altitude—in highly irradiated atmospheres.

This thesis investigates the atmospheric composition of the ultra-hot Jupiter WASP-189 b using high-resolution transmission spectroscopy, which probes a planet's atmosphere by analysing starlight filtered through it during transit. A key result is the first unambiguous detection of TiO in the transmission spectrum of an ultra-hot Jupiter, confirmed through observations with multiple high-resolution spectrographs. Given the high signal-to-noise observations of the system, WASP-189 b serves as an ideal benchmark for atmospheric characterisation.

This thesis also presents a wide chemical inventory of its optical transmission spectrum using both the cross-correlation technique and narrow-band spectroscopy, based on observations taken with HARPS, HARPS-N, ESPRESSO, and MAROON-X. Additionally, time-resolved absorption signals from these methods offer insights into the planet's atmospheric variations over the course of the transit.

Beyond ultra-hot Jupiters, this work explores the limitations of high-resolution transmission spectroscopy for warm Jupiters—gas giants on longer orbits where slower orbital velocities complicate atmospheric signal extraction. This analysis highlights the role of orbital configuration in the success of these techniques and identifies systems where observations remain feasible with current and future instruments. As exoplanet characterisation advances toward cooler planets in search of molecules such as carbon monoxide and water, overcoming these methodological challenges will be crucial for constraining elemental abundance ratios and linking atmospheric composition to planetary formation and migration histories.

Key words
Spectroscopy; exoplanets; exoplanet atmospheres; gas giants

Classification system and/or index terms (if any)		
Supplementary bibliographical information		**Language** English
ISSN and key title		**ISBN** ISBN: 978-91-8104-360-0 (print) ISBN: 978-91-8104-361-7 (pdf)
Recipient´s notes	**Number of pages** 221	**Price**
	Security classification	

Signature: **Date:** 2025-03-25

High-Resolution Transmission Spectroscopy of Gas Giant Atmospheres

Bibiana Prinoth

LUND UNIVERSITY

Faculty Opponent

Prof. Dr. Neale Gibson
School of Physics, Trinity College Dublin
Dublin, Ireland

Evaluation Committee

Dr. Michiel Lambrechts
Center for Star and Planet Formation and Natural History Museum of Denmark, Globe Institute, University of Copenhagen
Copenhagen, Denmark

Dr. Elna Heimdal Nilsson
Division of Combustion Physics, Department of Physics, Lund University
Lund, Sweden

Prof. Dr. Malcolm Fridlund
Department of Space, Earth and Environment, Chalmers University of Technology, Onsala Space Observatory
Onsala, Sweden

Cover: Artistic impression of the ultra-hot Jupiter WASP-189 b. I designed the graphics for the press release accompanying the publication of Prinoth et al. 2022, Paper I, included in this thesis.

Funding information: This thesis work is financially supported by the Royal Physiographic Society of Lund through the Walter Gyllenberg Foundation.

Faculty of Science, Department of Physics

ISBN: 978-91-8104-360-0 (print)
ISBN: 978-91-8104-361-7 (pdf)

Printed in Sweden by Media-Tryck, Lund University, Lund 2025

Für meinen kleinen Bruder Luca

Contents

List of publications

This thesis is based on the following peer-reviewed publications:

I **Titanium oxide and chemical inhomogeneity in the atmosphere of the exoplanet WASP-189 b**
Prinoth, Bibiana; Hoeijmakers, H. Jens; Kitzmann, Daniel; Sandvik, Elin; Seidel, Julia V.; Lendl, Monika; Borsato, Nicholas W.; Thorsbro, Brian; Anderson, David R.; Barrado, David; Kravchenko, Kateryna; Allart, Romain; Bourrier, Vincent; Cegla, Heather M.; Ehrenreich, David; Fisher, Chloe; Lovis, Christophe; Guzmán-Mesa, Andrea; Grimm, Simon; Hooton, Matthew; Morris, Brett M.; Oreshenko, Maria; Pino, Lorenzo; Heng, Kevin
Nature Astronomy, Volume 6, p. 449-45 (2022)

II **Time-resolved transmission spectroscopy of the ultra-hot Jupiter WASP-189 b**
Prinoth, Bibiana; Hoeijmakers, H. Jens; Pelletier, Stefan; Kitzmann, Daniel; Morris, Brett M.; Seifahrt, Andreas; Kasper, David; Korhonen, Heidi H.; Burheim, Madeleine; Bean, Jacob L.; Benneke, Björn; Borsato, Nicholas W.; Brady, Madison; Grimm, Simon L.; Luque, Rafael; Stürmer, Julian; Thorsbro, Brian
Astronomy & Astrophysics, Volume 678, id.A182, 38 pp. (2023)

III **An atlas of resolved spectral features in the transmission spectrum of WASP-189 b with MAROON-X**
Prinoth, Bibiana; Hoeijmakers, H. Jens; Morris, Brett M.; Lam, Madeline; Kitzmann, Daniel; Sedaghati, Elyar; Seidel, Julia V.; Lee, Elspeth K. H.; Thorsbro, Brian; Borsato, Nicholas W.; Damasceno, Yuri C.; Pelletier, Stefan; Seifahrt, Andreas
Astronomy & Astrophysics, Volume 685, id.A60, 33 pp. (2024)

IV **High-resolution transmission spectroscopy of warm Jupiters: An ESPRESSO sample with predictions for ANDES**
Prinoth, Bibiana; Sedaghati, Elyar; Seidel, Julia V.; Hoeijmakers, H. Jens; Brahm, Rafael; Thorsbro, Brian; Jordán, Andrés
The Astronomical Journal, Volume 168, Number 3 (2024)

Works not included in the thesis

Peer-reviewed publications not included in this thesis (in chronological order):

I **3D Radiative Transfer for Exoplanet Atmospheres. gCMCRT: A GPU-accelerated MCRT Code**
Lee, Elspeth K. H.; Wardenier, Joost P.; **Prinoth, Bibiana**; Parmentier, Vivien; Grimm, Simon L.; Baeyens, Robin; Carone, Ludmila; Christie, Duncan; Deitrick, Russell; Kitzmann, Daniel; Mayne, Nathan; Roman, Michael; Thorsbro, Brian
The Astrophysical Journal, Volume 929, Issue 2, id.180, 15 pp. (2022)

II **The Mantis Network II: examining the 3D high-resolution observable properties of the UHJs WASP-121b and WASP-189b through GCM modelling**
Lee, Elspeth K. H.; **Prinoth, Bibiana**; Kitzmann, Daniel; Tsai, Shang-Min; Hoeijmakers, Jens; Borsato, Nicholas W.; Heng, Kevin
Monthly Notices of the Royal Astronomical Society, Volume 517, Issue 1, pp.240-256 (2022)

III **The Mantis Network I: A standard grid of templates and masks for cross-correlation analyses of ultra-hot Jupiter transmission spectra**
Kitzmann, Daniel; Hoeijmakers, H. Jens; Grimm, Simon L.; Borsato, Nicholas W.; Lueber, Anna; **Prinoth, Bibiana**
Astronomy & Astrophysics, Volume 669, id.A113, 22 pp. (2023)

IV **The Mantis Network. III. Expanding the limits of chemical searches within ultra-hot Jupiters: New detections of Ca I, V I, Ti I, Cr I, Ni I, Sr II, Ba II, and Tb II in KELT-9 b**
Borsato, Nicholas W.; Hoeijmakers, H. Jens; **Prinoth, Bibiana**; Thorsbro, Brian; Forsberg, Rebecca; Kitzmann, Daniel; Jones, Kathryn; Heng, Kevin
Astronomy & Astrophysics, Volume 669, id.A113, 22 pp. (2023)

V **Vanadium oxide and a sharp onset of cold-trapping on a giant exoplanet**
Pelletier, Stefan; Benneke, Björn; Ali-Dib, Mohamad; **Prinoth, Bibiana**; Kasper, David; Seifahrt, Andreas; Bean, Jacob L.; Debras, Florian; Klein, Baptiste; Bazinet, Luc; Hoeijmakers, H. Jens; Kesseli, Aurora Y.; Lim, Olivia; Carmona, Andres; Pino, Lorenzo; Casasayas-Barris, Núria; Hood, Thea; Stürmer, Julian
Nature, Volume 619, Issue 7970, p.491-494 (2023)

VI **Detection of atmospheric species and dynamics in the bloated hot Jupiter WASP-172 b with ESPRESSO**
Seidel, Julia V.; **Prinoth, Bibiana**; Knudstrup, Emil; Hoeijmakers, H. Jens; Zanazzi, John J.; Albrecht, Simon
Astronomy & Astrophysics, Volume 678, id.A150, 10 pp. (2023)

VII **Small but mighty: High-resolution spectroscopy of ultra-hot Jupiter atmospheres with compact telescopes. Transmission spectrum of KELT-9 b with Wendelstein's FOCES spectrograph**
Borsato, Nicholas W.; Hoeijmakers, H. Jens; Cont, David; Kitzmann, Daniel; Ehrhardt, Jan; Gössl, Claus; Ries, Christoph; **Prinoth, Bibiana**; Molaverdikhani, Karan; Ercolano, Barbara; Kellerman, H; Heng, Kevin
Astronomy & Astrophysics, Volume 683, id.A98, 15 pp. (2024)

VIII **The Mantis Network IV: A titanium cold trap on the ultra-hot Jupiter WASP-121 b**
Hoeijmakers, H. Jens; Kitzmann, Daniel; Morris, Brett M.; **Prinoth, Bibiana**; Borsato, Nicholas W.; Thorsbro, Brian; Pino, Lorenzo; Lee, Elspeth K. H.; Akın, Can; Seidel, Julia V.; Birkby, Jayne L.; Allart, Romain; Heng, Kevin
Astronomy & Astrophysics, Volume 685, id.A139, 22 pp. (2024)

IX **Atmospheric characterization and tighter constraints on the orbital misalignment of WASP-94 A b with HARPS**
Ahrer, Eva-Maria; Seidel, Julia V.; Doyle, L.; Gandhi, Siddarth; **Prinoth, Bibiana**; Cegla, Heather M.; McDonald, C. H.; Astudillo-Defru, N.; Ayache, E.; Nealon, R.; Veras, Dimitri; Wheatley, P. J.; Ehrenreich, David
Monthly Notices of the Royal Astronomical Society, Volume 530, Issue 3, pp.2749-2759 (2024)

X **The atmospheric composition of the ultra-hot Jupiter WASP-178 b observed with ESPRESSO**
Damasceno, Yuri C.; Seidel, Julia V.; **Prinoth, Bibiana**; Psaridi, Angelica; Esparza-Borges, Emma; Stangret, Monika; Santos, Nuno C.; Zapatero-Osorio, Maria R.; Alibert, Yann; Allart, Romain; Azevedo Silva, Tomas; Cointepas, Marion; Costa Silva, Ana R.; Cristo, Eduardo; Di Marcantonio, Paolo; Ehrenreich, David; González Hernández, Jonay I.; Herrero-Cisneros, Eva; Lendl, Monika; Lillo-Box, J.; Martins, Carlos J. A. P.; Micela, Giuseppa; Pallé, Enric; Sousa, Sérgio G.; Steiner, Michal; Vaulato, Valentina; Zhao, Yinan; Pepe, Francesco
Astronomy & Astrophysics, Volume 689, id.A54, 18 pp. (2024)

XI **Secrets in the shadow: High precision stellar abundances of fast-rotating A-type exoplanet host stars through transit spectroscopy**
Lam, Madeline B.; Hoeijmakers, H. Jens; **Prinoth, Bibiana**; Thorsbro, Brian
Astronomy & Astrophysics, Volume, 691. id.A141, 13 pp. (2024)

XII **CRIRES+ and ESPRESSO reveal an atmosphere enriched in volatiles relative to refractories on the ultra-hot Jupiter WASP-121 b**
Pelletier, Stefan; Benneke, Björn; Chachan, Yayaati; Bazinet Luc; Allart, Romain; Hoeijmakers, H. Jens; Lavail, Alexis; **Prinoth, Bibiana**; Coulombe, Louis-Philippe; Lothringer, Joshua D.; Parmentier, Vivien; Smith, Peter; Borsato, Nicholas W.; Thorsbro, Brian
The Astronomical Journal, Volume 169, Issue 1, id.10, 16 pp. (2025)

XIII **Vertical structure of an exoplanet's atmospheric jet stream**
Seidel, Julia V.; **Prinoth, Bibiana**; Pino, Lorenzo; dos Santos, Leonardo A.; Chakraborty, Hritam; Sedaghati, Elyar; Wardenier, Joost P.; Farret Jentink, Casper; Zapatero Osorio, Maria Rosa; Allart, Romain; Ehrenreich, David; Parmentier, Vivien; Lendl, Monika; Roccetti, Giulia; Damasceno, Yuri C.; Bourrier, Vincent; Lillo-Box, Jorge; Pallé, Enric; Santos, Nuno; Suárez Mascareño, Alejandro; Sousa, Sergio G., Tabernero, Hugo M.; Pepe, Francesco
Nature, Volume 639, Issue 8056, p.902-908 (2025)

XIV **Titanium chemistry of WASP-121 b with ESPRESSO's 4-UT mode**
Prinoth, Bibiana; Seidel, Julia V.; Hoeijmakers, H. Jens; Morris, Brett M.; Baratella, Martina; Borsato Nicholas W.; Damasceno Yuri C.; Parmentier Vivien; Kitzmann Daniel; Sedaghati Elyar; Pino Lorenzo; Borsa, Francesco; Allart Romain; Santos Nuno; Steiner Michal; Suárez Mascareño, Alejandro; Tabernero, Hugo M.; Zapatero Osorio, Maria Rosa
Astronomy & Astrophysics, Volume 694, id.A284, 14 pp. (2025)

XV **Hot Rocks Survey I : A shallow eclipse for LHS 1478 b**
August, Prune C.; Buchhave, Lars A.; Diamond-Lowe Hannah; Mendonça João M.; Gressier, Amélie; Rathcke, Alexander D.; Allen, Natalie H.; Fortune, Mark; Jones Kathryn D.; Meier Valdés, Erik A.; Demory Brice-Olivier; Espinoza, Néstor; Fisher, Chloe E.; Gibson, Neale P.; Heng, Kevin; Hoeijmakers, H. Jens; Hooton, Matthew J.; Kitzmann, Daniel; **Prinoth, Bibiana**; Eastman, Jason D.; Barnes, Rory
Astronomy & Astrophysics, Volume 695, id.A171, 15 pp. (2025)

Popular summary

Research on the atmospheres of exoplanets – and astronomy in general – deals with extremes. One of these extremes is the distance to the objects we study – located so far away that even their light takes hundreds, or even thousands of years to reach us. Even light from the Sun takes about eight minutes to reach Earth. So, when we observe the Sun, we are seeing it as it was eight minutes ago. This time delay is just a small example of the vast distances we are working with when studying objects beyond our planet and Solar System.

On the other hand, the information that I find most intriguing comes from incredibly small sources: atoms and molecules in the atmospheres of exoplanets. When a planet passes in front of its star – a phenomenon called a planetary transit – some of the star's light is filtered through the planet's atmosphere. During this process, atoms and molecules leave distinct "fingerprints" – spectral lines – that allow us to decode the chemical composition of the atmospheres of distant worlds. This is exactly the focus of my dissertation, with a particular emphasis on the atmospheres of gas giant planets.

The planet I have focused on the most in my dissertation is the ultra-hot Jupiter WASP-189 b. It is located over 300 light-years away in the constellation Libra and orbits its star in just three days, making it one of the hottest planets known. If your eyesight is better than mine, you might even be able to spot its star on a dark and clear night. Because of the planet's short orbit, which causes it to travel around its star at over 200 km/s, it is relatively easy to detect the atmospheric "fingerprints" of atoms and molecules.

For my dissertation, I used observations of WASP-189 b with several spectrographs on telescopes around the world. By comparing the observed spectra with model predictions, it was possible to detect a number of metals – including iron, titanium, manganese, and even barium. One of the key discoveries was titanium oxide in the atmosphere of WASP-189 b. This molecule behaves similarly to ozone in our own atmosphere and causes a temperature inversion due to interaction with UV radiation, which warms up the atmosphere at higher altitudes. Titanium oxide has been notoriously difficult to detect over the years, but in the case of WASP-189 b, everything fell into place.

Just when I thought I was finished with WASP-189 b, I found an unexpected pattern in the data: spectral lines of ionised calcium in the planet's atmosphere. This led me to search for other known spectral lines, such as the Fraunhofer lines and the brightest spectral line from excited hydrogen (the Hα line). These lines probe the upper layers of the planet's atmosphere and can be identified without needing to compare them to models. This resulted in an atlas of these spectral lines in WASP-189 b 's atmosphere, which will hopefully serve as an important resource for testing models of atmospheric chemistry.

As my research progressed, the focus shifted to cooler planets (but still pretty warm), the so-called "warm Jupiters". These planets orbit their stars at greater distances, which makes studying their atmospheres more challenging due to their longer orbital periods. Their lower orbital velocities make it harder to isolate spectral lines. However, my research has shown that for planets with eccentric orbits, certain configurations allow us to still extract atmospheric information. For these cooler exoplanets, molecules like water and carbon monoxide provide clues about how these planets may have formed and ended up in their current orbits – a central question in exoplanet research. My final study highlights promising objects for future observations, and hopefully, these observations will one day contribute to solving the puzzle of how planets form.

Populärvetenskaplig sammanfattning

Forskning om exoplaneters atmosfärer – och egentligen astronomi i allmänhet – är studier om extrema förhållanden. En av dessa extremer är avståndet till objekten vi studerar – så pass avlägsna att deras ljus tar hundratals, ja till och med tusentals år för att nå oss. Även ljuset från solen tar cirka åtta minuter att nå jorden. Det vill säga, när vi observerar solen ser vi den som den var för åtta minuter sedan. Denna fördröjning ger perspektiv på de enorma avstånd vi hanterar när vi studerar objekt bortom vår planet och vårt solsystem.

Å andra sidan kommer informationen som enligt mig är mest intressant från otroligt små källor: atomer och molekyler i exoplaneternas atmosfärer. När en planet passerar framför sin stjärna – ett fenomen som kallas planetpassage – filtreras en del av stjärnljuset genom planetens atmosfär. Under denna process lämnar atomer och molekyler distinkta "fingeravtryck" – spektrallinjer – som gör det möjligt för oss att tyda den kemiska sammansättningen av atmosfärer hos avlägsna världar. Detta är exakt vad min avhandling fokuserar på, med särskild inriktning på gasjättars atmosfärer.

Den planet jag har arbetat med mest i min avhandling är den ultraheta Jupiter-liknande planeten WASP-189 b. Den ligger över 300 ljusår bort i stjärnbilden Vågen och kretsar kring sin stjärna på bara tre dagar – vilket gör den till en av de hetaste planeterna vi känner till. Om du har bättre syn än jag kan du kanske till och med få en skymt av dess stjärna under en mörk och klar natt. Tack vare planetens korta omloppstid, som får den att färdas över 200 km/s runt sin stjärna, är det relativt enkelt att känna igen de atmosfäriska "fingeravtrycken" från atomer och molekyler.

I min avhandling har jag använt observationer av WASP-189 b med flera spektrografer på teleskop runt om i världen. Genom att jämföra de observerade spektrumen med modeller gick det att upptäcka en rad metaller – inklusive järn, titan, mangan och till och med barium. En höjdpunkt var upptäckten av titanoxid i WASP-189 b:s atmosfär. Denna molekyl fungerar liknande som ozon i vår egen atmosfär och orsakar en temperaturinversion genom interaktion med UV-strålning, vilket värmer upp de högre lagerna av atmosfären. Titanoxid har visat sig vara svår att upptäcka, men i fallet med WASP-189 b föll alla bitarna på plats.

Just när jag trodde att jag var klar med WASP-189 b upptäckte jag ett oväntat mönster i datan: spektrallinjer av joniserat kalcium i planetens atmosfär. Detta ledde till en jakt efter andra kända spektrallinjer, såsom Fraunhoferska linjerna och den starkaste spektrallinjen från exciterat väte (Hα-linjen). Dessa linjer gör det möjligt att karaktärisera de höga lagren i planetens atmosfär och kan identifieras utan att behöva jämföras med modeller. Denna studie ledde till en atlas över dessa spektrallinjer i WASP-189 b:s atmosfär, som förhoppningsvis kommer att bli en viktig resurs för att verifiera modeller av atmosfärisk kemi.

Min forskning har över tid förskjutits mot kallare planeter, så kallade "varma Jupiter-liknande planeter". Dessa planeter kretsar kring sina stjärnor på längre avstånd än de heta planeterna, vilket gör att analysen av deras atmosfärer blir mer utmanande på grund av längre omloppstider. Hastigheten de rör sig runt sina stjärnor med är mycket lägre, vilket gör det svårare att isolera spektrallinjer. Min forskning har dock visat att för planeter med excentriska omloppsbanor gör vissa konfigurationer det möjligt för oss att extrahera atmosfärsinformation ändå. För dessa kallare exoplaneter ger molekyler som vatten och kolmonoxid ledtrådar om hur dessa planeter kan ha bildats och hamnat i sina nuvarande omloppsbanor – en central fråga inom exoplanetsforskning. Min sista studie lyfter fram lovande objekt för framtida observationer – och förhoppningsvis kommer dessa observationer en dag att bidra till att lösa pusslet om hur planeter bildas.

Populärwissenschaftliche Zusammenfassung

Die Forschung an den Atmosphären von Exoplaneten – und eigentlich die Astronomie im Allgemeinen – ist eine Wissenschaft der Extreme. Eines dieser Extreme ist die Entfernung zu den von uns untersuchten Objekten – die sich soweit weg befinden, dass ihr Licht Hunderte oder sogar Tausende von Jahren braucht, um uns zu erreichen. Selbst das Licht der Sonne braucht etwa acht Minuten, um bei uns auf der Erde anzukommen. Wenn wir also die Sonne beobachten, sehen wir sie so, wie sie vor acht Minuten war. Diese Zeitverzögerung ist nur ein kleines Beispiel für die gewaltigen Entfernungen, mit denen wir es zu tun haben, wenn wir Objekte jenseits unseres Planeten und unseres Sonnensystems untersuchen.

Andererseits stammt die Information, die uns meiner Meinung nach am meisten interessiert, aus unglaublich kleinen Quellen: Atomen und Molekülen in den Atmosphären von Exoplaneten. Wenn ein Planet vor seinem Stern vorbeizieht – ein Phänomen, das als Planetendurchgang bezeichnet wird – wird ein Teil des Sternenlichts durch die Planetenatmosphäre gefiltert. Dabei hinterlassen Atome und Moleküle eindeutige "Fingerabdrücke" – Spektrallinien – die es uns ermöglichen, die chemische Zusammensetzung der Atmosphären ferner Welten zu entschlüsseln. Genau darauf konzentriert sich meine Dissertation, mit speziellem Fokus auf die Atmosphären von Gasriesen.

Der Planet, mit dem ich mich in meiner Dissertation am meisten befasst habe, ist der ultra-heisse Jupiter WASP-189 b. Er befindet sich über 300 Lichtjahre entfernt im Sternbild Waage und umkreist seinen Stern in nur drei Tagen – was ihn zu einem der heissesten Planeten macht, die wir bisher kennen. Wenn dein Sehvermögen besser ist als meines, kannst du vielleicht sogar einen Blick auf seinen Stern in einer dunklen und klaren Nacht erhaschen. Dank der kurzen Umlaufzeit des Planeten, die ihn mit über 200 km/s um seinen Stern rasen lässt, ist es relativ einfach, die atmosphärischen "Fingerabdrücke" von Atomen und Molekülen als solche zu erkennen.

In meiner Dissertation habe ich Beobachtungen von WASP-189 b mit mehreren Spektrografen auf Teleskopen rund um den Globus verwendet. Durch den Vergleich der beobachteten Spektren mit Modellvorhersagen war es möglich, eine Reihe von Metallen zu entdecken – darunter Eisen, Titan, Mangan und sogar Barium. Ein Höhepunkt war die Entdeckung von Titanoxid in der Atmosphäre von WASP-189 b. Dieses Molekül verhält sich ähnlich wie Ozon in unserer eigenen Atmosphäre und verursacht eine Temperaturumkehrung aufgrund der Wechselwirkung mit UV-Strahlung, die die Atmosphäre in höheren Lagen erwärmt. Titanoxid hat sich über die Jahre als schwer nachweisbar herausgestellt, aber im Fall von WASP-189 b fügte sich alles zusammen.

Gerade als ich dachte, ich wäre mit WASP-189 b fertig, entdeckte ich ein unerwartetes Muster in den Daten: die Spektrallinien von ionisiertem Kalzium in der Atmosphäre des Planeten. Dies führte zu einer Jagd nach anderen bekannten Spektrallinien, wie den Fraunhoferschen Linien und der hellsten Spektrallinie des angeregten Wasserstoffs (der Hα-Linie). Mit diesen Linien lassen sich die hohen Schichten der Planetenatmosphäre erforschen und sie können ohne den Vergleich mit Modellen identifiziert werden. Dies führte zu einem Atlas dieser Spektrallinien in der Atmosphäre von WASP-189 b, der hoffentlich eine wichtige Ressource für die Überprüfung von Vorhersagen zur atmosphärischen Chemie werden wird.

Im Laufe meiner Forschung verlagerte sich der Fokus auf kühlere Planeten, die sogenannten "warmen Jupiter". Diese Planeten umkreisen ihre Sterne in grösserem Abstand als ihre wärmeren Geschwister, wodurch die Analyse der Atmosphären dieser Planeten aufgrund der längeren Umlaufzeiten erschwert wird. Die Geschwindigkeit, mit der sie ihre Sterne umkreisen, ist viel niedriger, was es schwieriger macht, die Spektrallinien zu isolieren. Allerdings zeigte meine Arbeit, dass für Planeten mit exzentrischen Umlaufbahnen bestimmte Konfigurationen es uns ermöglichen, die atmosphärischen Informationen trotzdem zu extrahieren. Für diese kühleren Exoplaneten liefern Moleküle wie Wasser und Kohlenmonoxid Hinweise darauf, wie diese Planeten möglicherweise entstanden sind und in ihre heutigen Umlaufbahnen gelangt sind – eine zentrale Frage in der Exoplanetenforschung. Meine abschliessende Arbeit hebt vielversprechende Objekte für zukünftige Beobachtungen hervor – und eines Tages könnten diese Beobachtungen dazu beitragen, das Rätsel der Planetenentstehung zu entschlüsseln.

Résumé de vulgarisation scientifique

L'étude des atmosphères d'exoplanètes – et l'astronomie en général – touche à des extrêmes. L'un de ces extrêmes est la distance qui nous sépare des objets que nous étudions. Ils sont situés à des années-lumière, si loin que même leur lumière met des centaines, voire des milliers d'années à nous parvenir. Même la lumière émise par le Soleil met environ huit minutes pour parvenir à la Terre. Ainsi, lorsque nous observons le soleil, nous le voyons tel qu'il était il y a huit minutes. Ce délai temporel n'est qu'un petit exemple des distances colossales auxquelles nous sommes confrontés lorsque nous étudions des objets au-delà de notre planète et de notre Système solaire.

À l'inverse, les informations qui me semblent les plus fascinantes proviennent de sources minuscules : les atomes et les molécules dans les atmosphères des exoplanètes. Lorsqu'une planète passe devant son étoile – un phénomène appelé transit planétaire – une partie de la lumière émise par l'étoile traverse l'atmosphère de la planète. Au cours de ce processus, les atomes et molécules constituant l'atmosphère laissent des "empreintes" distinctes – des raies spectrales – qui nous permettent de décoder la composition chimique des atmosphères de ces mondes lointains. C'est exactement l'objectif de ma thèse, qui porte une attention particulière aux atmosphères des géantes gazeuses.

La planète qui se trouve au centre de ma thèse est la Jupiter ultra-chaude WASP-189 b. Elle est située à plus de 300 années-lumière de la Terre dans la constellation de la Balance et complète une orbite autour de son étoile en seulement trois jours, ce qui en fait l'une des planètes les plus chaudes connues. Si ton acuité visuelle est meilleure que la mienne, tu pourrais même peut-être apercevoir son étoile lors d'une nuit claire et sombre. En raison de sa période orbitale courte, procurant à la planète une vitesse de plus de 200 km/s, il est relativement facile de détecter les "empreintes" atmosphériques des atomes et des molécules.

Pour ma thèse, j'ai utilisé les données d'observations de WASP-189 b réalisées avec plusieurs spectrographes sur des télescopes à travers le monde entier. En comparant les spectres observés avec les prédictions des modèles, nous avons pu détecter plusieurs métaux – dont le fer, le titane, le manganèse et même le baryum. L'un des points les plus marquants fut la découverte d'oxyde de titane dans l'atmosphère de WASP-189 b. Cette molécule se comporte de manière similaire à l'ozone dans notre propre atmosphère et provoque une inversion de température de par son interaction avec le rayonnement ultraviolet, ce qui réchauffe l'atmosphère à des altitudes plus élevées. La détection de l'oxyde de titane a longtemps posé

beaucoup de difficultés, mais dans le cas de WASP-189 b, tout s'est accordé parfaitement.

Au moment même où je pensais en avoir terminé avec WASP-189 b, j'ai découvert un motif inattendu dans les données : des raies spectrales de calcium ionisé dans l'atmosphère de la planète. Cela m'a amenée à chercher d'autres raies spectrales connues, telles que les raies de Fraunhofer et la raie spectrale la plus brillante de l'hydrogène excité (la raie Hα). Ces raies sondent les couches supérieures de l'atmosphère de la planète et peuvent être identifiées sans nécessiter une comparaison aux modèles. Mon travail a abouti à un atlas de ces raies spectrales dans l'atmosphère de WASP-189 b, qui, je l'espère, servira de ressource importante pour tester les modèles de chimie atmosphérique.

Au fil de l'avancement de ma recherche, l'accent s'est progressivement tourné vers des planètes plus froides (mais toujours assez chaudes), appelées "Jupiters tièdes". Ces planètes se trouvent sur des orbites plus éloignées autour de leurs étoiles, ce qui rend l'étude de leurs atmosphères plus difficile en raison du prolongement de leurs périodes de révolution. Leurs vitesses orbitales plus faibles compliquent l'isolement des raies spectrales. Cependant, ma recherche prouve que pour les planètes ayant des orbites excentriques, certaines configurations permettent tout de même d'extraire des informations sur l'atmosphère. Pour ces exoplanètes plus froides, des molécules comme l'eau et le monoxyde de carbone fournissent des indices sur les mécanismes de formation de ces planètes et comment elles se sont retrouvées sur leurs orbites actuelles – une question centrale de la recherche sur les exoplanètes. Mon étude finale met en évidence des objets prometteurs pour les futures observations, et j'espère que ces observations contribueront un jour à résoudre l'énigme de la formation des planètes.

Sintesi di divulgazione scientifica

La ricerca sulle atmosfere degli esopianeti – e sull'astronomia in generale – riguarda lo studio di oggetti estremi. Uno degli aspetti più estremi dello studio degli esopianeti è la loro distanza: sono così lontani che persino la loro luce impiega centinaia, se non migliaia di anni per raggiungerci. Basti pensare alla luce del Sole, che impiega circa otto minuti per arrivare sulla Terra. Questo significa che, quando osserviamo il Sole, lo vediamo com'era otto minuti fa. Questo ritardo temporale è solo un piccolo esempio delle immense distanze con cui abbiamo a che fare quando studiamo corpi celesti al di là del nostro pianeta e al di fuori del Sistema Solare.

D'altra parte, ciò che trovo più affascinante nello studio degli esopianeti proviene da fonti incredibilmente piccole: gli atomi e le molecole nelle loro atmosfere. Quando un pianeta passa davanti alla sua stella – un fenomeno chiamato transito – parte della luce stellare viene filtrata attraverso l'atmosfera del pianeta. Durante questo processo, gli atomi e le molecole lasciano delle "impronte digitali" uniche – linee spettrali – che ci permettono di decifrare la composizione chimica dell'atmosfera di pianeti lontani. Questo è esattamente il tema della mia tesi, con un focus particolare sulle atmosfere dei pianeti giganti gassosi.

Il pianeta su cui mi sono concentrata maggiormente nella mia tesi è il Giove ultra-caldo WASP-189 b. Situato a oltre 300 anni luce di distanza, nella costellazione della Bilancia, orbita intorno alla sua stella in soli tre giorni, rendendolo uno dei pianeti più caldi conosciuti. Se la tua vista fosse migliore della mia, potresti persino individuare la sua stella in una notte buia e limpida. A causa della sua orbita breve, , che lo porta a ruotare intorno alla stella a oltre 200 km/s, è relativamente semplice rilevare le "impronte digitali" atmosferiche di atomi e molecole.

Per la mia tesi, ho utilizzato osservazioni di WASP-189 b effettuate con diversi spettrografi su telescopi sparsi in tutto il mondo. Confrontando gli spettri osservati con le previsioni dei modelli teorici, sono riuscita a identificare numerosi metalli, tra cui ferro, titanio, manganese e perfino bario. Una delle scoperte più rilevanti è stata la presenza di ossido di titanio nell'atmosfera di WASP-189 b. Questa molecola si comporta in modo simile all'ozono nella nostra atmosfera e causa un'inversione termica dovuta all'interazione con la radiazione ultravioletta, che riscalda gli strati più alti dell'atmosfera. L'ossido di titanio è stato storicamente difficile da rilevare, ma nel caso di WASP-189 b, tutto è andato per il verso giusto.

Proprio quando pensavo di aver concluso lo studio su WASP-189 b, ho individuato un pattern inaspettato nei dati: linee spettrali di calcio ionizzato nell'atmosfera del pianeta. Questo mi ha spinta a cercare altre linee spettrali note, come le linee di Fraunhofer e la linea spettrale più brillante dell'idrogeno eccitato (la linea Hα). Queste linee permettono di sondare gli strati più alti dell'atmosfera del pianeta e possono essere identificate direttamente, senza bisogno di confrontarle con i modelli teorici. Il risultato è stata la creazione di un atlante di linee spettrali nell'atmosfera di WASP-189 b, che spero diventi una risorsa importante per testare i modelli di chimica atmosferica.

Proseguendo con la mia ricerca, l'attenzione si è spostata verso pianeti più freddi (ma comunque abbastanza caldi), i cosiddetti "Giovi tiepidi". Questi pianeti orbitano a distanze maggiori dalle loro stelle, il che rende lo studio delle loro atmosfere più complesso a causa dei periodi orbitali più lunghi. Inoltre, le loro velocità orbitali più basse rendono più difficile isolare le linee spettrali. Tuttavia, la mia ricerca ha dimostrato che, per i pianeti con orbite eccentriche, alcune configurazioni permettono comunque di estrarre informazioni atmosferiche. Per questi esopianeti più freddi, molecole come l'acqua e il monossido di carbonio offrono indizi su come si siano formati e su come abbiano raggiunto le loro orbite attuali – una delle questioni centrali nella ricerca sugli esopianeti. Il mio ultimo studio ha individuato alcuni oggetti promettenti per future osservazioni, e spero che queste indagini possano un giorno contribuire a risolvere l'enigma della formazione di questi pianeti.

Resumen de divulgación científica

La investigación sobre las atmósferas de exoplanetas – y la astronomía en general – trata de los extremos. Uno de estos extremos es la enorme distancia a la que se encuentran los objetos que estudiamos. Están tan lejos que su luz puede tardar cientos, e incluso miles, de años en alcanzarnos. Para ponerlo en perspectiva, la luz del Sol tarda aproximadamente ocho minutos en llegar a la Tierra. Por lo cual, cuando observamos el Sol, estamos viéndolo como era hace ocho minutos. Este retraso temporal es solo un pequeño ejemplo de las enormes distancias con las que trabajamos al estudiar objetos más allá de nuestro planeta y nuestro Sistema Solar.

Por otro lado, la información que encuentro más fascinante proviene de fuentes diminutas: los átomos y las moléculas en las atmósferas de los exoplanetas. Cuando un planeta pasa frente a su estrella – un fenómeno conocido como tránsito – parte de la luz estelar atraviesa la atmósfera del planeta. Durante este proceso, los átomos y las moléculas dejan "huellas digitales" únicas – líneas espectrales – que nos permiten descifrar la composición química de las atmósferas de mundos distantes. Este es precisamente el tema de mi tesis, con un enfoque particular en las atmósferas de los planetas gigantes gaseosos.

El planeta en el que más me he enfocado en mi tesis es el Júpiter ultra-caliente WASP-189 b. Se encuentra a una distancia de más de 300 años luz en la constelación de Libra y orbita su estrella en solo tres días, convirtiéndolo en uno de los planetas más calientes conocidos. Si tu vista fuera mejor que la mía, incluso podrías distinguir su estrella en una noche oscura y clara. Debido a la corta órbita del planeta, que lo hace viajar alrededor de su estrella a más de 200 km/s, es relativamente fácil detectar las "huellas digitales" atmosféricas de los átomos y las moléculas.

En mi tesis, utilicé observaciones de WASP-189 b con varios espectrógrafos en telescopios alrededor del mundo. Comparando los espectros observados con las predicciones de los modelos, fue posible detectar varios metales – incluyendo hierro, titanio, manganeso e incluso bario. Uno de los principales descubrimientos fue el óxido de titanio en la atmósfera de WASP-189 b. Esta molécula se comporta de manera similar al ozono en nuestra atmósfera y causa una inversión térmica debido a la interacción con la radiación ultravioleta, lo que calienta la atmósfera en alturas más elevadas. El óxido de titanio ha sido notoriamente difícil de detectar a lo largo de los años, pero en el caso de WASP-189 b, todo encajó perfectamente.

Justo cuando creía haber terminado con WASP-189 b, encontré un patrón inesperado en los datos: líneas espectrales de calcio ionizado en la atmósfera del planeta. Esto me llevó a buscar otras líneas espectrales conocidas, como las líneas de Fraunhofer y la línea espectral más brillante del hidrógeno excitado (la línea Hα). De estas líneas se puede extraer muestras de las capas superiores de la atmósfera del planeta y pueden identificarse sin necesidad de compararlas con modelos. Esto resultó en un atlas de estas líneas espectrales en la atmósfera de WASP-189 b, que espero sirva como un recurso importante para probar los modelos de química atmosférica.

A medida que avanzaba mi investigación, el enfoque se desplazó hacia planetas más fríos (pero aún bastante calientes), los llamados "Júpiteres tibios". Estos planetas orbitan sus estrellas a distancias más grandes, lo que hace que estudiar sus atmósferas sea más desafiante debido a sus períodos orbitales más largos. Sus velocidades orbitales más bajas dificultan el aislamiento de las líneas espectrales. Sin embargo, mi investigación ha mostrado que, para los planetas con órbitas excéntricas, ciertas configuraciones nos permiten aún extraer información atmosférica. En el caso de estos exoplanetas más fríos, moléculas como el agua y el monóxido de carbono proporcionan información sobre cómo pudieron formarse estos planetas y llegar en sus órbitas actuales – una pregunta central en la investigación de exoplanetas. Mi estudio final destaca objetos prometedores para futuras observaciones, y espero que estas observaciones ayuden algún día a resolver el rompecabezas de la formación de planetas.

Acknowledgements

It takes a village to do a PhD. And my village is probably more like a city by now. I will not be able to mention all of you here, but thank you for sticking with me for so long. Thank you for being my metropolis.

First and foremost, I want to thank my supervisors and mentors for believing in me, and forming me into the independent researcher I am today. Jens, for giving me the privilege of being your first PhD student, for letting me dive deep into the rabbit hole of titanium chemistry, and for your guidance throughout this journey. We started our Sweden-adventure at the same time, learnt to navigate the jungle of LU bureaucracy, and I would dare say we have succeeded in mastering basically everything thrown at us. Thank you for preparing me for the science world out there. Brian, for being our server god, whether you wanted it or not, and for showing me that it is okay to question decisions made by literally everyone – including and especially myself. David, for giving me the freedom to pursue whatever I wanted without question, but always reassuring others that I was doing great. Elyar, for pulling me out into the world, and showing me that there is more beyond little Europe and the shiny atmospheres of ultra-hot Jupiters. For believing in me and pushing me way before I even knew about it. Julia, for being an incredible mentor and inspiring role model, for letting me discover the wonders of your shiny 4-UT data – but most of all for showing me what it means to be a woman in science and teaching me how to navigate and succeed in this world. I'm looking forward to many more projects and cross-correlation to-do lists on whiteboards, aber auch Schlagernächte in München und carnevals in Nice.

To the exoplanet team: Jens, Brian, Nic, Stefan, Elin, Lucian, Aline, Alex, Ally, Klaudia, Lise, Lydia, Madeline, Brett, and those I missed during my time in Chile – thank you for making research a collaborative and inspiring adventure. For making me re-explain my train of thoughts, for feeding me with cookies, and for discussing science and pondering about what 'truth' even means.

To everyone at Lund Observatory, I won't be able to name you all. An enormous thanks to Daniel, Álvaro, Camilla, Isabella, and Victor, my office mates, who made everyday life more enjoyable, who listened to me talking to myself when thinking out loud, and made sure I drink water and not only coffee. Rebecca, you were the first role model I needed in my career, and you've become one of my closest friends. Linn and Madeleine, for our countless D&D – Dinner & Disney – evenings. Anka, for being an honorary member of the astrophysics division. For all the social adventures, especially the karaoke nights – *my heart will go on*.

To everyone who helped me get this monster of a thesis over the finish line: Xmas Girl, for walking me through your licentiate thesis and giving me an idea of what a thesis in Sweden even looks like. Brian, for basically trashing it (politely of course) and letting me rearrange it all. Julia, for making sure I don't accidentally invent processes in Earth's atmosphere. Rebecca, for fishing out my spelling mistakes – especially the embarrassing typos in the Swedish popular summary, for being probably one of the only few people to read this thing from top to bottom, and for convincing me that I need six popular science summaries. Kira, for saving me from my high-school French. Alain, Juan, Madeleine, and Julia, for making my Spanish summary sound better than my B1 – and confirming that we are indeed working with Júpiteres ultra-caliente and hidrógeno excitado. And Giulia, for reminding me once again that my Italian citizenship may be at risk if anyone reads the Italian version before your comments.

A mis chilen@s – Ana, Julia, Alejandro, Alain, Gustavo, Yuri, Micha, Elyar, Eli, Jaime, the cool office, the not-so-cool office, y much@s más – gracias por hacer que mi tiempo en Chile fuera la raja. Por hacerme sentir en casa, incluso cuando no cachaba ni una wea.

An meine Trüdels, die seit jeher mit dabei sind, mich in so vielen Phasen meines Lebens gesehen haben und sich trotzdem immer wieder entschieden haben, ein Teil davon zu sein und zu bleiben. Danke, dass ihr meine Liebe zur Wissenschaft immer voll unterstützt habt.

An meine ETH-schnuggis – Moji, Lara, Bene, Juju, Ramon, Viki, Jonas, Andreas, Jonas, Selina, Max und Lizzie – danke, dass ihr mein Anker gewesen seid. Moji, danke, dass du von Anfang an eine Schwester und mein Engel warst. Dafür, dass du immer an mich geglaubt hast, vor allem dann, wenn ich selbst an mir gezweifelt habe. Ich lieb' dich immer einmal mehr. Bene, dafür, dass du mir immer gezeigt hast, was im Studium und im Leben wirklich wichtig ist. Ich bin mir zu 100% sicher, dass ich ohne dich heute nicht da wäre, wo ich bin. Lara und Jonas, dafür, dass ihr es mit mir ausgehalten habt, in all meinen Phasen, mit mir Biene Maja getanzt und Corona-Frozen gesungen habt (Wir haben da immer noch den high score). Andreas, dafür, dass du mit mir die abgefahrensten Reisen gemacht hast und mich Teil deiner Familie hast sein lassen. *Egészségedre!* Viki, Ramon, Jonas, Moji und Andreas, dafür, dass es immer ganz viel food food food and love gegeben hat und immer geben wird.

An meine IDEALiStiC-er – Aline, Jannis und Corentin –, die mir gezeigt haben, dass Freundschaften zwar oft in einem professionellen Umfeld beginnen, sich aber darüber hinaus zu etwas Lebenslangem entwickeln könnnen.

An meinen Mathelehrer, Ulrich Kugler, der meine Liebe zur Wissenschaft gesehen hat und mich in die richtige Richtung geschubst hat.

An meine Familie – meine Eltern, Alexandra (merci maman), Helmuth, Daniela und Serge, sowie meine Geschwister, Luca, Luca und Romina – dafür, dass ihr das Fundament meines Dorfes seid. An meine Grosseltern, die mich bei jedem Schritt meines Weges unterstützt haben und stolz auf mich sind.

Till min svenska familj – Kerstin, Göran, Örjan, Simon, Christina, Eva, Sverker, Anette, Peter, Eric och min bästa vän Linn – som välkomnade en liten schweizisk tjej och fick Sverige att kännas som hemma.

And finally, to my love, Martin, who has stood by me through all the ups and downs. Thank you for loving me through my temperamental outbursts, laughter, tears, and crazy bike tours, for supporting me, and for being part of my adventures in both life and career.

Part I

Research context

Summary of Scientific Publications

My thesis concerns the study of ultra-hot and warm gas giant exoplanetary transmission spectra. I focus on the high-resolution transmission spectroscopy of the ultra-hot Jupiter WASP-189 b and extend this work to warm Jupiters with predictions for the ANDES high-resolution spectrograph, to be installed on ESO's Extremely Large Telescope.

Paper I: *Titanium oxide and chemical inhomogeneity in the atmosphere of the exoplanet WASP-189 b*

In this work, we study the optical high-resolution transmission spectrum of the ultra-hot Jupiter WASP-189 b based on observations with the HARPS and HARPS-N spectrographs. We search for absorption by atoms and molecules in the planet's transmission spectrum using the cross-correlation technique, detecting Fe, Fe^+, Ti, Ti^+, Cr, Mg, V, Mn, and TiO. Of particular interest is the detection of TiO, which has been the subject of debate with multiple claimed detections and refutations in ultra-hot Jupiter atmospheres. We further find that the line positions likely differ due to spatial gradients in their abundances, suggesting that they originate from different regions or dynamical regimes.

Paper II: *Time-resolved transmission spectroscopy of the ultra-hot Jupiter WASP-189 b*

In this work, we study the optical high-resolution transmission spectrum of the ultra-hot Jupiter WASP-189 b based on observations with the HARPS, HARPS-N, ESPRESSO, and MAROON-X spectrographs. We search for absorption by atoms and molecules using the cross-correlation technique. Thanks to the high signal-to-noise ratio obtained by stacking the planetary transits, the spectral traces are resolved in time. By fitting the orbital traces of the detected species using time-resolved spectroscopy, we infer posterior distributions for orbital parameters as well as line shapes. Our results indicate that different species must originate from different regions of the atmosphere to explain the observed time dependence of the signals. Finally, we confirm the detection of TiO in the transmission spectrum of WASP-189 b.

Paper III: *An atlas of resolved spectral features in the transmission spectrum of WASP-189 b with MAROON-X*

In this work, we study the high-resolution transmission spectrum of the ultra-hot Jupiter WASP-189 b based on observations with the MAROON-X spectrograph. Using differential transmission spectroscopy, we identify individual absorption lines of Ca^{+}, Ba^{+}, Na, Hα, Mg, Fe, and Fe^{+}. For the resolved Ca^{+} lines, we fit the planetary and stellar parameters by modelling the stellar spectrum behind the planet at each orbital phase during transit. We use this to correct for the Rossiter-McLaughlin effect imprinted on the transmission spectra.

Paper IV: *High-resolution transmission spectroscopy of warm Jupiters: An ESPRESSO sample with predictions for ANDES*

In this work, we study the high-resolution transmission spectra of six warm gas giants based on observations with the ESPRESSO spectrograph. Using the cross-correlation technique, we search for water absorption and report non-detections for all targets. These non-detections are partially attributed to the planets' typically small in-transit radial velocity changes, which make it difficult to distinguish between the different spectral components – the star, planet, Rossiter-McLaughlin effect, and telluric contamination – as well as the relatively weak planetary absorption lines compared to the signal-to-noise ratio of the spectra. We simulate observations with the upcoming high-resolution spectrograph ANDES at the Extremely Large Telescope for the two most favourable planets on eccentric orbits searching for water, carbon monoxide, and methane.

Chapter 1

Introduction

"If at first it doesn't make sense, it's a historical thing."

– Becky Smethurst, *A Brief History of Black Holes*

1.1 Motivation

The first detection of an atmosphere beyond Earth dates back to 1761, when Mikhail Lomonosov observed the transit of Venus and inferred its presence from the refraction of sunlight at the planet's limb (Marov 2004). This early observation hinted at the power of light to study atmospheres, but it would take a few more decades before spectroscopy systematically revealed their compositions. In 1814, Joseph von Fraunhofer mapped dark absorption lines in the solar spectrum (von Fraunhofer 1814), marking a key milestone in identifying chemical elements in stellar and planetary atmospheres. By the mid-20th century, spectroscopy had become a fundamental tool for planetary science, with ground-based observations revealing the primary constituents of the atmospheres of Venus, Mars, and the giant planets (Kuiper 1952).

Several more years would pass before exoplanets were discovered – not to mention the possibility that their atmospheres could be studied in great detail. The first suspected exoplanet discovery dates back to 1988 (around Gamma Cephei A, Campbell et al. 1988), though it remained unconfirmed for years (Hatzes et al. 2003). Meanwhile, Aleksander Wolszczan and Dale Frail announced the discovery of two terrestrial exoplanets around a very different kind of star than the Sun – the pulsar PSR B1257+12 (Wolszczan & Frail 1992). The first confirmed detection of an exoplanet around a Sun-like star then came in 1995 with the discovery of 51 Pegasi b. Swiss astronomers Michel Mayor and Didier Queloz detected the planet using the ELODIE spectrograph at the Observatoire de Haute-Provence in France (Mayor & Queloz 1995). Their groundbreaking discovery, which revealed the existence of gas giant planets orbiting extremely close to their host stars – so-called hot Jupiters – was honoured with the 2019 Nobel Prize in Physics for their contributions to our understanding of planetary systems and Earth's place in the cosmos.

What once seemed like a distant possibility – studying the atmospheres of planets outside our Solar System – became tangible with the discovery of transiting exoplanets. The hot Jupiter HD 209458 b became the first known planet observed passing in front of its star (Charbonneau et al. 2000), allowing direct measurements of its size, and later, its atmosphere. In 2002, Charbonneau et al. (2002) identified sodium absorption in the planet's transmission spectrum, marking the first detection[1] of an exoplanetary atmosphere and proving that transmission spectroscopy could reveal the chemical composition of distant worlds – a technique specifically predicted to succeed for this kind of planets (Seager & Sasselov 2000; Brown 2001; Hubbard et al. 2001).

Since then, hot Jupiters – and their even more extreme siblings, ultra-hot Jupiters – have remained key targets in exoplanet atmosphere studies. These gas giants, with orbital periods shorter than 10 days, reside about 100 times closer to their stars than Earth does to the Sun. For the hottest of them, the intense irradiation from their host stars drives temperatures beyond 2 000 K, creating an environment where molecules thermally dissociate, atomic and ionic chemistry dominates, and strong atmospheric dynamics shape their structure and composition (e.g. Fortney et al. 2021). Despite being relatively rare, these extreme environments are a treasure trove for atmospheric characterisation, revealing a plethora of metals like iron, titanium and vanadium in gas form (see e.g. Hoeijmakers et al. 2018, 2019).

This thesis focuses on one such target: the ultra-hot Jupiter WASP-189 b (Papers I–III). The following chapters provide the background for understanding the current exoplanet population, leading into the study of their atmospheres and the observational and analysis techniques used to infer their chemical composition. Each method has its intrinsic limitations, which become increasingly apparent as we push toward cooler planets (Paper IV).

[1] To stir some controversy early on: High-resolution ground-based observations later suggested that stellar effects could also explain (parts of) this absorption (Casasayas-Barris et al. 2021).

1.2 Exoplanet detection methods

Today, 30 years after the ground-breaking discovery of 51 Pegasi b, nearly 6000 exoplanets have been identified.[2] The vast majority of these planets have been discovered using indirect methods that rely on detecting changes in the velocity or brightness of their host stars.

Radial velocity. 51 Pegasi b was discovered through one of the most widely used indirect methods: through monitoring the radial velocity of its host star – the motion of the star towards or away from the observer. In the early days, this technique was employed to study binary star systems, which consist of two stars orbiting a common centre of mass. With advancements in instrumentation and data analysis, it became feasible to adapt this method for detecting exoplanets, which are orders of magnitude less massive than stars (e.g. Wright 2018).

In its roots, the radial velocity method exploits basic physics: the movement of two (or more) bodies around a common centre of mass – the barycentre. For the Solar System, this position may vary from being close to the centre of the Sun to outside its surface, governed by the position of the planets relative to each other. The dominant influence is exerted by Jupiter being the most massive body in the Solar System apart from the Sun. Additionally, the other three gas giants, Saturn, Uranus, and Neptune, also have an effect on the position of the barycentre, while the inner rocky planets are negligible. It is this gravitational tug-of-war between a planet (or several) and its host star that makes it possible for us to detect (some of) these planets in the first place.

When observing an exoplanet's host star, its movement around the common centre of mass will cause the spectral lines of the stellar atmosphere to be Doppler-shifted compared to where we would expect them if the star were stationary, see Figure 1.1. This shift in wavelength corresponds to a velocity shift, which we call the radial velocity of the host star because it represents the velocity component along our line of sight from Earth – either toward us or away from us.

The radial velocity of the star $v_{\mathrm{RV},*}(t)$ in its most general form is given by

$$v_{\mathrm{RV},*}(t) = K_* \left[\cos\left(\theta(t) + \omega\right) + \varepsilon \cos\left(\omega\right)\right] + v_{\mathrm{system}}, \tag{1.1}$$

where K_* is the radial velocity semi-amplitude of the star depending on planetary and stellar properties, see Equation (1.2); $\theta(t)$ is the true anomaly, which describes

[2] There are 5 839 confirmed exoplanets based on the NASA Exoplanet Archive, retrieved on February 25, 2025.

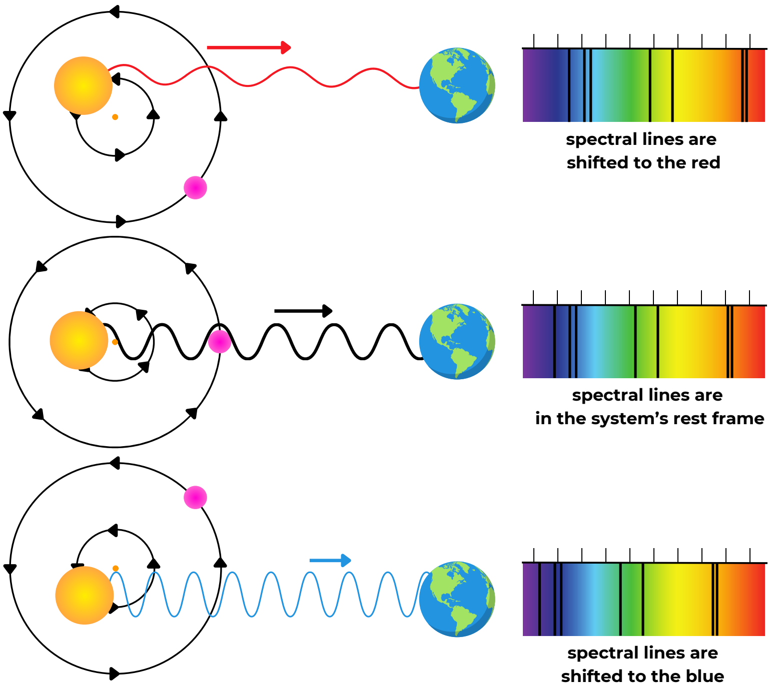

Figure 1.1: Radial velocity method schematic. When the star moves towards us, the spectra lines are blue-shifted compared to the stationary lines in the system's rest frame. If it moves away from us, they are red-shifted. Schematic is exaggerated for visualisation purposes.

the position of the planet on its orbit as a function of time, see Figure 1.2; ω is the argument of periastron, which describes the angle at which the planet and star are at their closest approach; ε is the orbital eccentricity; and v_{system} is the systemic velocity, i.e. the radial velocity of the system's centre of mass. The radial velocity semi-amplitude K_* is given by

$$K_* = \left(\frac{2\pi G}{P}\right)^{1/3} \frac{M_p \sin{(i)}}{(M_* + M_p)^{2/3}} \frac{1}{\sqrt{1-\varepsilon^2}}, \tag{1.2}$$

where G is the gravitational constant, P is the orbital period of the planet, M_p is the mass of the planet, M_* is the mass of the star; and i is the inclination of the orbit relative to the line of sight, see Figure 1.2. For a full derivation of Equation (1.2), see Lovis & Fischer (2010).

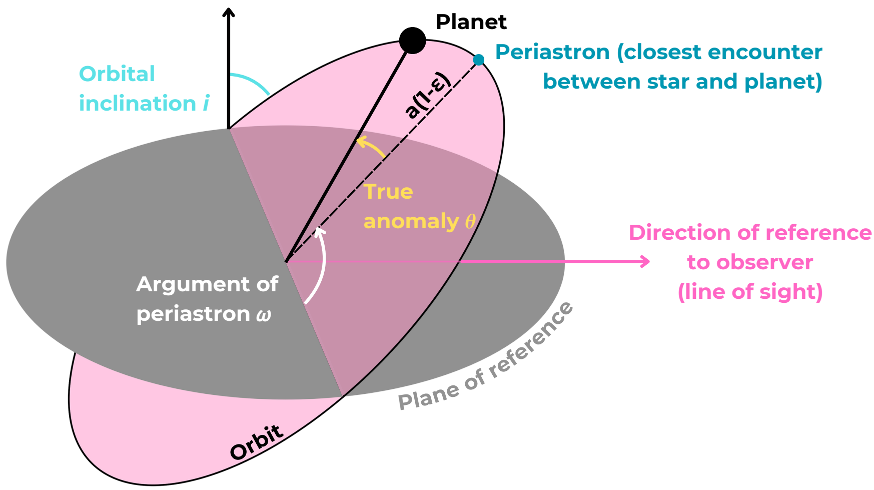

Figure 1.2: Relevant orbital elements for exoplanets. Figure inspired by Sun et al. (2022). In the case of a circular orbits ($\varepsilon = 0$), the periastron occurs in the direction of the observer, i.e. at $\omega = 90$ deg.

For a given star with mass M_*, the radial velocity semi-amplitude is larger for smaller periods P, heavier planets M_p, and edge-on orbits ($i = 90\,\mathrm{deg}$). This naturally highlights the observational bias associated with the radial velocity technique towards heavy planets on close-in, edge-on orbits. Furthermore, the radial velocity method only provides a measurement for the minimal mass of the planet, as one only measures $M_p \sin i$ and not M_p directly. Thus, follow-up observations may reveal that the planet is indeed more massive.

Transit method. A large fraction of the exoplanets discovered today have been detected using the transit method, particularly due to the launch of the Kepler mission in 2009 (Borucki et al. 2010). If a planet moves in front of its host star when observed from Earth, this results in a dimming of the brightness of the star, proportional to the area covered by the planet, see Figure 1.3. The drop in brightness is called the transit depth δ, given by

$$\delta = \frac{A_p}{A_*} = \frac{\pi R_p^2}{\pi R_*^2} = \frac{R_p^2}{R_*^2}, \tag{1.3}$$

where A_p and A_*, and R_p and R_* are the effective projected area and radius of the planet and the star, respectively.

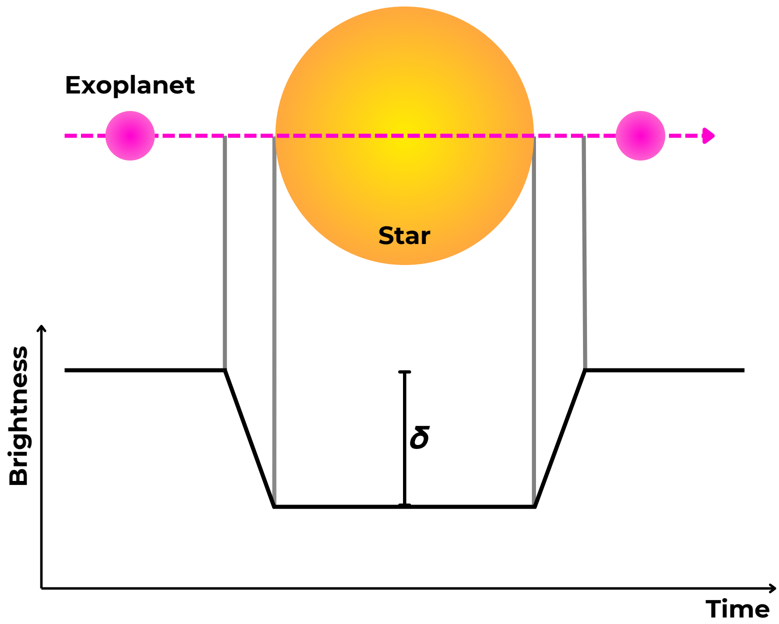

Figure 1.3: Schematic transit light curve. As the exoplanet moves in front of the star, the brightness is dimmed proportional to the area of the star covered by the planet.

If this drop in brightness occurs periodically, this may indicate the presence of a planet around the host star. Similar to the radial velocity method, transits are biased towards planets with short orbital periods, and large radii. Periodicity of the signal is a stringent requirement for a signal to become a candidate for an exoplanet. However, the signal of other phenomena may also be periodic in time, such as for example stellar variability. Thus, transit observations are prone to false-positives or -alarms, and a confirmation via radial velocity observations is needed to confirm or refute the planetary nature of a signal.

Other methods

While transit and radial velocity measurements account for the vast majority of exoplanets discovered to date and form the foundation of the core techniques on which this thesis is based (see Chapter 3), several other methods exist for detecting exoplanets. For completeness, these are briefly described here.

Direct imaging. A significant milestone came in 2004, when the first direct detection of an exoplanet was achieved using the NACO adaptive optics instrument on the European Southern Observatory's Very Large Telescope (Chauvin et al. 2004). This detection was subsequently confirmed in 2005 with additional data collected using the same instrument (Chauvin et al. 2005). Direct imaging captures light directly from the planet, either from its thermal emission or reflected starlight (see e.g. Currie et al. 2023, for a review). Unlike transit or radial velocity measurements, this method directly detects the planet itself rather than relying on changes of the host star. It is, however, limited to targets that are at large separations from their host stars. Instruments that are currently being upgraded, particularly GRAVITY+, will extend the sensitivity to planets orbiting closer to their host stars (Gravity+ Collaboration et al. 2022).

Astrometry. While the radial velocity technique detects exoplanets by measuring their motion along the observer's line of sight, there two additional velocity components that describe the motion in the plane of the sky, and these form the basis of astrometric observations. This method detects exoplanets by measuring small positional shifts of a star in the plane of the sky caused by the gravitational pull of an orbiting planet (Wright & Gaudi 2013). Only recently, the Gaia satellite detected its first exoplanets using astrometry, confirmed through radial velocity measurements (Sozzetti et al. 2023; Stefánsson et al. 2025). This breakthrough is expected to lead to thousands of additional detections by Gaia in the coming years (Perryman et al. 2014).

Microlensing. When a foreground star moves in front of a more distant background star, the gravitational field of the foreground star bends and magnifies the background star's light — a phenomenon known as gravitational lensing (Einstein 1936). If the foreground star hosts a planet, the planet's own gravitational field can create a detectable contribution to the lensing effect (Mao & Paczynski 1991; Gould & Loeb 1992; Tsapras 2018). Microlensing is particularly effective at detecting exoplanets at orbital separations of around 1–10 au (Gaudi et al. 2002; Gould et al. 2010), making it a valuable complement to other detection methods. However, a key limitation is that microlensing events are one-time occurrences, as the precise alignment of stars does not repeat. The first successful detection of an exoplanet through microlensing dates back to 2003 with the OGLE and MOA survey (Bond et al. 2004), which played a pioneering role in identifying these rare events. Looking ahead, future missions like the Nancy Grace Roman Space Telescope have microlensing as one of their key objectives (Penny et al. 2019; Johnson et al. 2020), promising to expand our census of exoplanets at intermediate orbital distances.

Transit Timing Variations (TTVs). While the transit method relies on periodic dips in a star's brightness caused by a planet passing in front of it, deviations from strict periodicity can indicate the presence of additional planets. These variations arise from gravitational interactions between planets, which alter their orbits and affect transit timing (Holman & Murray 2005; Agol et al. 2005). TTVs are especially useful for detecting additional non-transiting planets (e.g Kepler-9 and Kepler-19 systems, Holman et al. 2010; Ballard et al. 2011) and constraining planetary masses in multi-planet systems (e.g. the TRAPPIST-1 system, Gillon et al. 2017).

1.3 Exoplanet population

The known exoplanet population today includes nearly 6000 planets, thanks to the methods described above, and a few others not covered here for conciseness. However, only around 250 exoplanets have confirmed atmospheric detections[3]. As we will see in the following chapters, detecting and characterising exoplanetary atmospheres relies heavily on understanding orbital elements, as well as stellar and planetary parameters. The majority of these atmospheric detections stem from transiting planets on short orbital periods, where their atmospheres can be probed using transmission spectroscopy – a concept introduced in Chapter 3. Figure 1.4 shows the current exoplanet population and the subset with atmospheric detections, as of February 5, 2025. The apparent lack of planets in the lower-right region of the plot reflects the limited sensitivity of current instrumentation, which makes it difficult to detect planets on longer orbits with smaller masses.

[3]According to the ExoAtmospheres database (Instituto de Astrofísica de Canarias), retrieved on February 5, 2025.

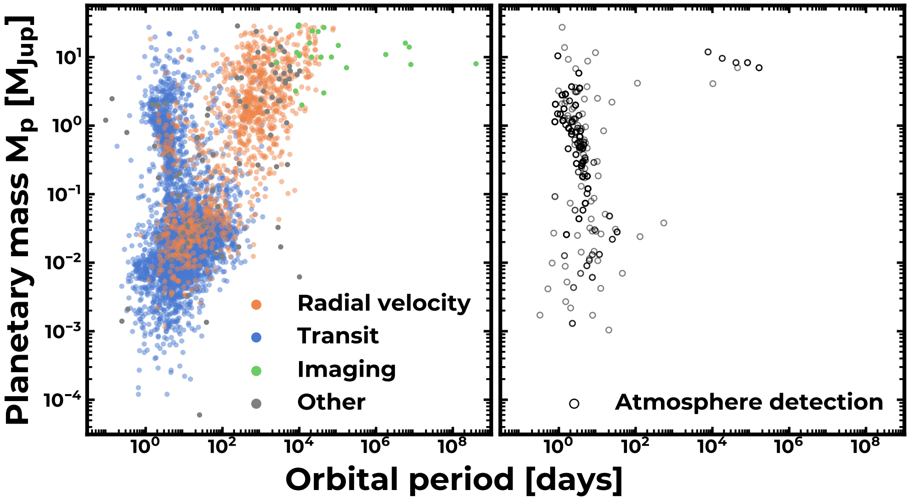

Figure 1.4: Exoplanet population and atmospheric detections as of February 5, 2025. *Left:* Exoplanet population from the `pscomppars` table of the NASA Exoplanet Archive. Planetary mass (in Jupiter masses) is plotted against orbital period (in days). Colours indicate detection methods: radial velocity (blue), transits (orange), imaging (green), and other (grey). **Right:** Planets with detected atmospheres from the ExoAtmospheres database.

Chapter 2

Planetary atmospheres

"We, all of us, are what happens when a primordial mixture of hydrogen and helium evolves for so long that it begins to ask where it came from."

– Jill Tarter, *former director of the Center for SETI Research*

Planetary atmospheres are inherently complex, governed by a variety of physical and chemical processes. The key parameters that describe an atmosphere – pressure, temperature, and composition – ultimately determine how light interacts with it. Even within our own Solar System, atmospheric properties vary widely from planet to planet (Visscher 2022). For example, Jupiter's atmosphere is dominated by hydrogen and helium, with methane as a key tertiary component (Niemann et al. 1998). Saturn's atmosphere shares a similar composition (Fletcher et al. 2009), while the inner Solar System presents a stark contrast: Earth's atmosphere is primarily nitrogen, whereas Venus' atmosphere is dominated by carbon dioxide (Adams & Dunham 1932; Adel & Slipher 1934). It is therefore not surprising that this diversity also extends to exoplanetary atmospheres.

Nevertheless, certain simplifying assumptions can be made when studying atmospheric properties. These assumptions help us describe the structure and composition of planetary atmospheres in a consistent and tractable way. This chapter provides an overview of these atmospheric characteristics, placing them in the context of Earth's atmosphere and exploring the expectations for hot and ultra-hot Jupiters.

2.1 Structure and composition

For the purposes of this thesis, atmospheres are assumed to be one-dimensional (plane-parallel) and in hydrostatic, thermal, and chemical equilibrium. These assumptions impose constraints on the atmospheric structure, particularly on pressure and temperature, as well as its composition.

2.1.1 Pressure

Hydrostatic equilibrium ensures that a planet's atmosphere remains gravitationally bound, neither escaping into space nor collapsing under its own weight. In a one-dimensional atmosphere, this balance is expressed as

$$\frac{\mathrm{d}P}{\mathrm{d}z} = -\rho g, \tag{2.1}$$

where g is the gravitational acceleration, P is the pressure, and ρ is the gas density. Assuming the gas behaves like an ideal gas, the pressure is given by

$$P = \rho R T = \rho \frac{k_\mathrm{B}}{m_u} T, \tag{2.2}$$

where R is the specific gas constant, k_B is the Boltzmann constant, and m_u is the mean molecular weight. Solving Equation (2.1) then leads to

$$P = P_0 \exp\left(-z/H\right), \tag{2.3}$$

where $H = \frac{k_B T}{m_u g}$ is the pressure scale height and P_0 is the reference pressure at the bottom of the atmosphere.

The pressure scale height provides a measure of how "puffy" an atmosphere is, whereas higher temperatures, lower mean molecular weights, and weaker gravitational pull all lead to a larger scale height. To put this in perspective, the pressure scale height of Earth is $H_\mathrm{Earth} \approx 8\,\mathrm{km}$, while for Jupiter, it is $H_\mathrm{Jupiter} \approx 27\,\mathrm{km}$. In comparison, a hot gas giant planet with approximate values of $T = 2\,500\,\mathrm{K}$, $g = 20\,\mathrm{m\,s^{-2}}$, $m_u = 2.3\,\mathrm{u}$ (assuming an atmosphere dominated by hydrogen and helium), has a scale height of $H_\mathrm{hot} \approx 450\,\mathrm{km}$. This large scale height makes hot gas giants particularly well-suited for observations via transmission spectroscopy (see Chapter 3).

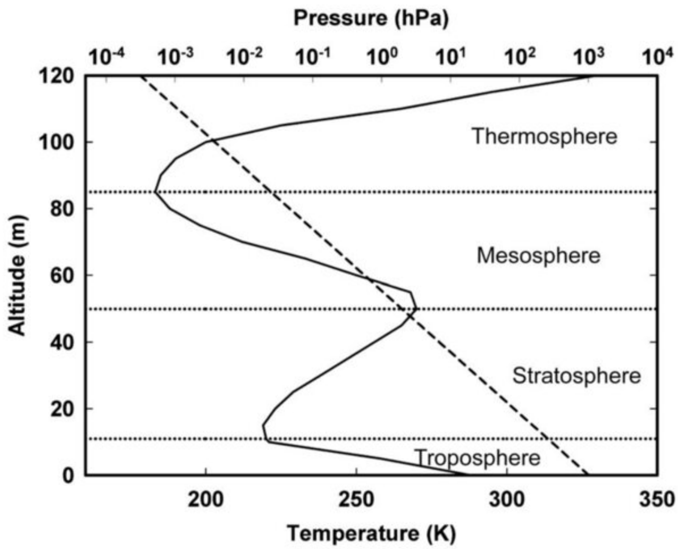

Figure 2.1: Temperature (solid) and pressure (dashed) structure of Earth's atmosphere. Figure from (Ahrens 1994) with permission.

2.1.2 Temperature

Temperature is a fundamental property of planetary atmospheres, shaping both their physical structure and chemical composition. It governs the pressure scale height in Equation (2.3) and determines which species can remain in the gas phase. At the same time, temperature itself depends on atmospheric composition, creating a strong link between thermal and chemical processes. Understanding an atmosphere's temperature structure is therefore essential, as it influences dynamics, chemistry, and energy transport across different altitudes and pressures. The complexity of atmospheric temperature profiles is well illustrated by Earth's atmosphere (Figure 2.1). Notably, the temperature increases in the stratosphere due to the interaction of UV radiation with ozone, a process known as the Chapman cycle.

In the absence of detailed observations, planetary atmospheres are often assumed to be in thermal equilibrium, maintaining radiative balance between incoming (stellar) and outgoing (planetary) radiation. A common simplification is to model the atmosphere as isothermal at the planet's equilibrium temperature $T_{\rm eq}$. This theoretical value represents the temperature a planet would reach if both

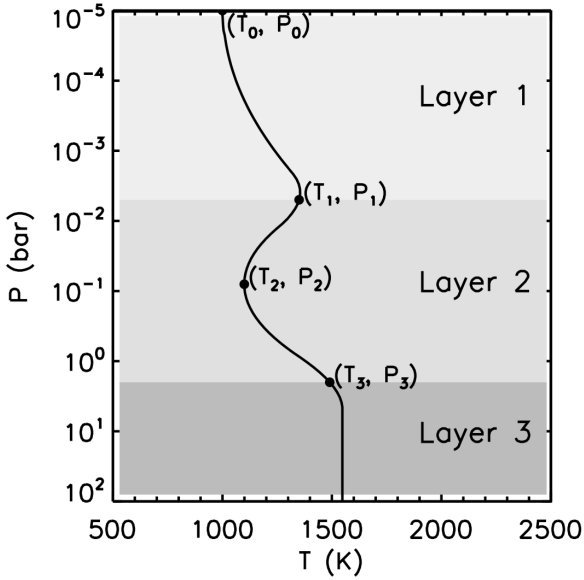

Figure 2.2: The parametric temperature-pressure profile from Madhusudhan & Seager (2009) introducing vertical stratification via three layers. ©AAS. Reproduced with permission.

the star and planet radiated as black bodies, following the Stefan-Boltzmann law ($F_{\rm BB} = k_{\rm B}T^4$, where T is the temperature of the star or planet). The equilibrium temperature is given by

$$T_{\rm eq} = T_* \sqrt{\frac{R_*}{2a}} (1 - A_B)^{1/4}, \tag{2.4}$$

where T_* is the star's effective temperature, R_* its radius, a the planet's semi-major axis, and A_B the Bond albedo, quantifying the planet's reflectivity.

For Earth ($T_{\rm eff,\odot} = 5\,780$ K, $R_* = R_\odot$, $a = 1$ au, $A_B \approx 0.3$), this results in an equilibrium temperature of $T_{\rm eq} = 255$ K, below the freezing point of water. While this estimate approximates Earth's average temperature (Figure 2.1), it significantly underestimates Venus' temperature. Due to Venus' CO_2-dominated atmosphere and strong greenhouse effect (Kasting 1988), its actual surface temperature is about 500 K higher than its equilibrium temperature of 226 K.

Although the assumption of an isothermal atmosphere is an oversimplification, it often suffices to describe current observations of transmission spectra (see Section 2.3). A more refined approach involves parametrising the atmosphere with multiple layers (e.g. Madhusudhan & Seager 2009), similar to the stratified structure of Earth's atmosphere. This allows for features like temperature inversions and more complex vertical profiles (Figure 2.2).

2.1.3 Chemistry

The other key factor influencing the pressure scale height in Equation (2.3) is the mean molecular weight, which depends on atmospheric composition. Composition varies with altitude due to differences in transport and chemical processes. Figure 2.3 shows Earth's approximate atmospheric composition as a function of altitude. The dominant species are molecular nitrogen (N_2) and oxygen (O_2), followed by carbon dioxide (CO_2), all of which are constant in abundance over the considered pressure range. In contrast, water vapour (H_2O) is more abundant at lower altitudes/higher pressures, because its upward transport is limited by atmospheric circulation (Palchetti et al. 2008, and references therein).

Earth's atmosphere is in constant exchange with its surface, influenced by both natural processes and human activity. This dynamic interaction leads to temporal variations in molecular abundances, making the atmosphere a complex four-dimensional system. Figure 2.3 approximates this system in one dimension for the purpose of studying Earth as an exoplanet (e.g. Lustig-Yaeger et al. 2023)

As previously highlighted, gas giant atmospheres are dominated by hydrogen and helium (Visscher 2022). A small fraction of the atmospheric composition is then made up of molecules and atoms, depending on the temperature and pressure structure. In Jupiter, a relatively cold gas giant, methane is the next dominant compound, whereas hotter gas giants, like ultra-hot Jupiters, are known to host refractory elements like iron in the gas phase, see Chapter 4.

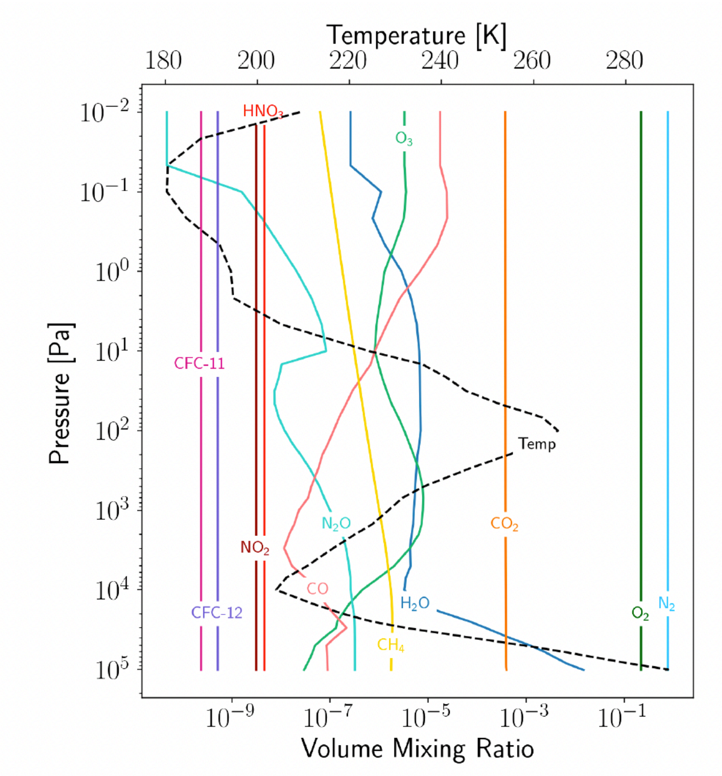

Figure 2.3: Approximate 1D thermal structure and composition of Earth's atmosphere from Lustig-Yaeger et al. (2023), licensed under CC BY 4.0.

2.2 Radiative transfer

The composition of a planetary atmosphere determines how it interacts with light. The key quantity governing this interaction is the optical depth τ, which describes how much light is absorbed or scattered as it passes through the atmosphere. The (dimensionless) optical depth τ is defined as

$$\tau = \int n\sigma dx = \int nm\kappa dx, \tag{2.5}$$

where n is the number density of the absorbing or scattering species (number of particles per unit volume), σ is the cross-section (effective area for interaction), m is the mass, κ is the opacity (cross-section per unit mass), and x represents the optical path of the light[1].

The optical depth $\tau \sim 1$ marks the photosphere, the last emitting layer in an atmosphere observed in emission, and the deepest layer where light is extinguished during a transit. An atmosphere is considered transparent or optically thin when $\tau \ll 1$, and opaque or optically thick when $\tau \gg 1$.

Number densities are derived from the volume mixing ratios, i.e., the chemical abundances described earlier. The cross-sections (and thus the opacities κ) depend on wavelength and reflect the likelihood that photons will interact with specific atmospheric species. These interactions, whether through absorption or scattering, imprint distinct spectral signatures on the observed light.

2.2.1 Opacity sources

The dominant opacity sources in an atmosphere arise from atomic and molecular absorption, scattering processes, and various continuum effects. In Earth's atmosphere, major molecular absorbers include water vapor (H_2O), carbon dioxide (CO_2), methane (CH_4), and ozone (O_3), with prominent absorption bands in the infrared and ultraviolet, see Figure 2.4 for infrared cross-sections.

In addition to line absorption from individual species, several continuum processes shape atmospheric opacity. Rayleigh scattering by neutral molecules — mainly N_2 and O_2 on Earth — increases opacity at short wavelengths (e.g. Rayleigh 1899). Collision-induced absorption arises from temporary interactions between molecular pairs like N_2-N_2 and N_2-O_2 (Frommhold 1994), enhancing infrared absorption in dense atmospheric layers (e.g. Farmer 1966).

[1] In practice, the total optical depth is obtained by summing contributions from individual absorbing and scattering components.

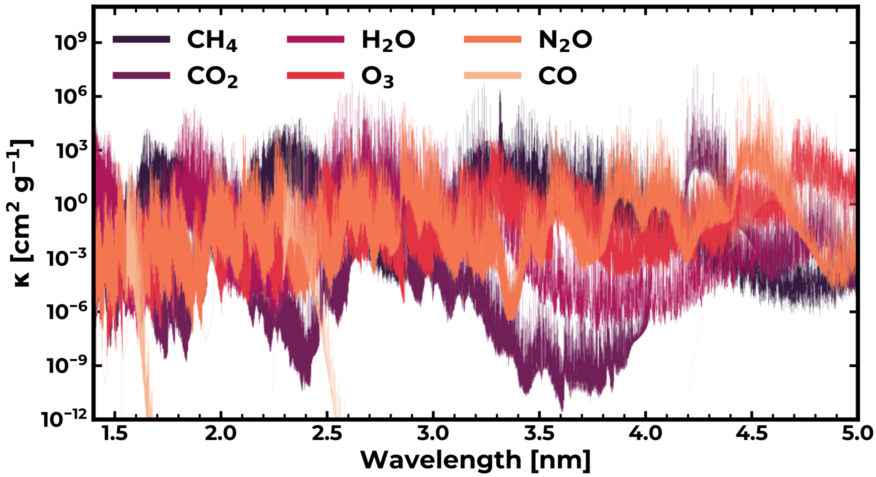

Figure 2.4: Absorption cross sections σ of the dominant molecular opacity sources in Earth's atmosphere at $T = 300\,\mathrm{K}$ and $p = 1\,\mathrm{hPa} = 10^{-3}$ bar. Opacities from the DACE Opacity Database.

Clouds and aerosols further complicate radiative transfer by contributing broadband opacity through scattering and absorption. Water clouds in Earth's troposphere significantly affect the planet's energy balance (Palchetti et al. 2008), while the reaction of sulphate aerosols – particularly sulphur dioxide, which often originates from volcanic eruptions – with water vapour in the stratosphere can lead to long-term climate impacts (e.g. Symons 1888, this link was first clearly established after the Krakatoa eruption in Indonesia in 1883). Unlike relatively well-characterised atomic and molecular opacity, cloud contributions may vary widely with altitude, composition, and particle size, adding complexity to atmospheric models that we yet have to fully understand.

2.2.2 Planetary spectrum

To derive the observable spectrum of an exoplanet from the atmospheric optical depth, one must solve the radiative transfer equation

$$\mu \frac{\partial I}{\partial \tau} = I - S, \tag{2.6}$$

where μ is the cosine of the incident angle, I is the intensity, and S is the source function. This equation governs the propagation of light through an atmosphere, accounting for both absorption and scattering processes. The source function, S, describes the emission of radiation from the medium and is typically a function of temperature, pressure, and the nature of the medium.

Solving the radiative transfer equation requires approximations due to the complexity of the source function S (Heng & Marley 2018). One common assumption is *local thermal equilibrium* (LTE), where the source function S is given by the Planck function, $S = B_\lambda(T)$, with T being the local temperature of the atmosphere. In this case, S depends only on the temperature and is independent of the radiation's angle μ.

Alternatively, one might neglect the contribution of the source function entirely, assuming that the planet's thermal emission is minimal and only the absorption of incoming stellar light is important. This leads to a simplified form of the radiative transfer equation

$$\mu \frac{\partial I}{\partial \tau} = I, \tag{2.7}$$

which has the solution

$$I = I_* \exp(-\tau/\mu), \tag{2.8}$$

where I_* is the intensity of the host star. This equation is known as *Beer's law*, which describes how the intensity of light passing through the exoplanetary atmosphere is exponentially attenuated.

2.3 Exoplanet context

One of the most intriguing discoveries, alongside the detection of planets orbiting stars other than the Sun, is the emergence of a class of planets unlike any in the Solar System: hot and ultra-hot Jupiters. These were the first planets discovered around main-sequence stars (Mayor & Queloz 1995), and thanks to their large scale heights (see Equation 2.3), their atmospheres are particularly well suited for characterisation. Before discussing how to observe these targets, it is worthwhile to first consider the extreme conditions shaping their atmospheres due to their close proximity to their stars.

Their short orbital separations subject them to extreme irradiation, fundamentally altering their atmospheric composition and dynamics. Due to strong gravitational interactions with their host stars, these planets are expected to become tidally locked – similar to the Moon-Earth configuration – soon after formation (Arras & Socrates 2010). As a result, their atmospheres are divided into a permanently irradiated, intensely heated dayside and a cooler, perpetually dark nightside. Dayside temperatures can exceed 2 000 K, leading to thermal dissociation of most molecules and partial ionisation of atomic species (Lothringer et al. 2018; Kitzmann et al. 2018; Parmentier et al. 2018; Arcangeli et al. 2018). On the much cooler nightside, atoms are expected to recombine into molecules (e.g., H_2 recombination, Bell & Cowan 2018), and complex processes such as cloud formation, condensation, rain-out, and cold trapping of certain elements can confine species to deeper atmospheric layers (e.g. Spiegel et al. 2009; Helling et al. 2021; Komacek & Showman 2016).

This interplay of temperature and chemistry bears some resemblance to processes seen closer to home. Much like the ozone-driven temperature inversions in Earth's stratosphere caused by the Chapman cycle, titanium and vanadium oxides have been hypothesised to drive similar inversions on the daysides of ultra-hot Jupiters (i.e., the side always facing the star, e.g. Hubeny et al. 2003; Fortney et al. 2006, 2008; Burrows et al. 2008; Parmentier et al. 2015). Yet despite these predictions, observational studies often appear to favour simpler atmospheric structures when observed in transit – when the planet passes in front of its host star and probes the atmospheric limbs, see Chapter 3 – where retrieved temperature-pressure profiles frequently favour isothermal structures (e.g. Gibson et al. 2022; Gandhi et al. 2023, and Figure 2.5). This motivates the widespread use of isothermal temperature assumptions in both detection and atmospheric retrieval studies of transit observations.

In ultra-hot Jupiters, H^- bound-free and free-free transitions often dominate the continuum opacity, particularly on the intensely heated dayside where hydrogen ionisation is more efficient (e.g. Wishart 1979; Bell & Berrington 1987; Arcangeli et al. 2018; Lothringer et al. 2018; Parmentier et al. 2018; Kitzmann et al. 2018). Alongside molecular absorption by species like H_2O, CO, and

CH_4, metals remain in the gas phase due to the high temperatures and absorb significantly, see Chapter 4 for specific detections.

At high pressures, collision-induced absorption from H_2-H_2 and H_2-He interactions becomes an important opacity source. Clouds and hazes further complicate the modelling of these atmospheres, with condensates like silicates and sulphides forming in the cooler regions of exoplanetary atmospheres (e.g. Marley et al. 2013). In this thesis, clouds are mentioned for completeness but have not been included in the analysis of the planets studied.

Interpreting the transmission and emission spectra of exoplanets requires accurate opacity data, which are compiled in extensive line lists cataloguing cross-sections of species relevant to exoplanetary atmospheres. These line lists are made available through databases such as `VALD` (Piskunov et al. 1995), `ExoMol` (Yurchenko & Tennyson 2014; Tennyson et al. 2016), and `HITRAN` (Rothman et al. 2013). Using these line lists, wavelength-dependent opacities κ [$\mathrm{cm}^2\,\mathrm{g}^{-1}$] can be computed, accounting for temperature and pressure effects.

To efficiently incorporate these line opacities into radiative transfer calculations, precomputed opacity tables, such as those provided by the DACE Opacity Database from `HELIOS-K` (Grimm & Heng 2015; Grimm et al. 2021), allow rapid interpolation over temperature, pressure, and species abundances. Radiative transfer (including retrieval) codes commonly used in exoplanetary science include `petitRADTRANS` (Mollière et al. 2019), `CHIMERA` (Line et al. 2013), and `HELIOS-R2` (`BeAR`, Kitzmann et al. 2020; Kitzmann & Grimm 2022). These codes adopt different approaches to solving the radiative transfer equation, producing planetary spectra that encapsulate atmospheric composition, temperature structure, and planetary parameters.

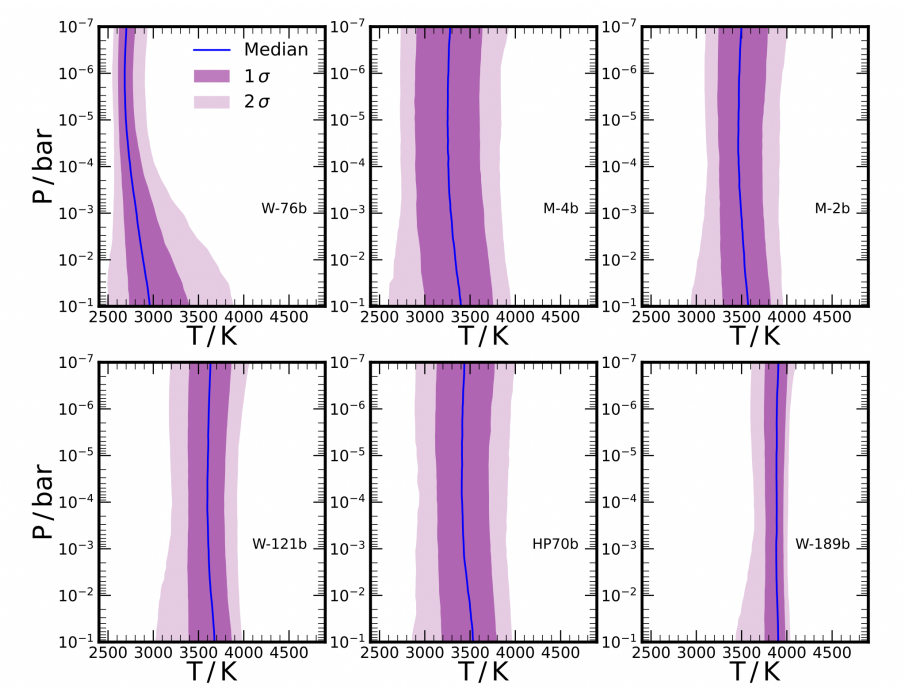

Figure 2.5: Retrieved temperature profiles for six ultra-hot Jupiters from Gandhi et al. (2023), licensed under CC BY 4.0.

Chapter 3

Transmission spectroscopy

"Looking through the atmosphere is like looking through a piece of old stained glass. The glass has defects that distort the image. The atmosphere also has defects that distort the image, but the defects in the atmosphere move, thus blurring the image as well. The glass is colored, so only some colors get through."

– Nancy Grace Roman, *"The Gestation of the Hubble"*

Directly observing the spectrum, and therefore the atmosphere, of an exoplanet is an extremely challenging task. Exoplanets are inherently faint compared to their host stars, rendering both their detection and atmospheric characterisation difficult. Furthermore, their close proximity to the star (often sub-arcsecond separations) challenges our ability to resolve the planet and star as distinct components. To date, this has only been successful for widely separated companions in young systems, where the planets are still relatively hot and emit significant infrared radiation (e.g. Macintosh et al. 2015; Chauvin et al. 2017; Picos et al. 2024; Zhang et al. 2024; Gandhi et al. 2025).

However, early studies have leveraged the favourable geometries of transiting planets (e.g. Charbonneau et al. 2002). During a transit, starlight passes through the upper layers of the atmosphere, where it undergoes partial absorption or scattering before reaching the telescope. This interaction causes a portion of the light to be blocked by optically thick regions, and another portion to be filtered through optically thin layers. Crucially, the planet's apparent radius – defined as the radius where the planet's atmosphere becomes optically thick – varies with wavelength governed by the absorbing atoms and molecules. Observations of this wavelength-dependent radius result in transmission spectra, which can be used to probe the planet's atmospheric properties (Seager & Sasselov 2000), see Chapter 2.

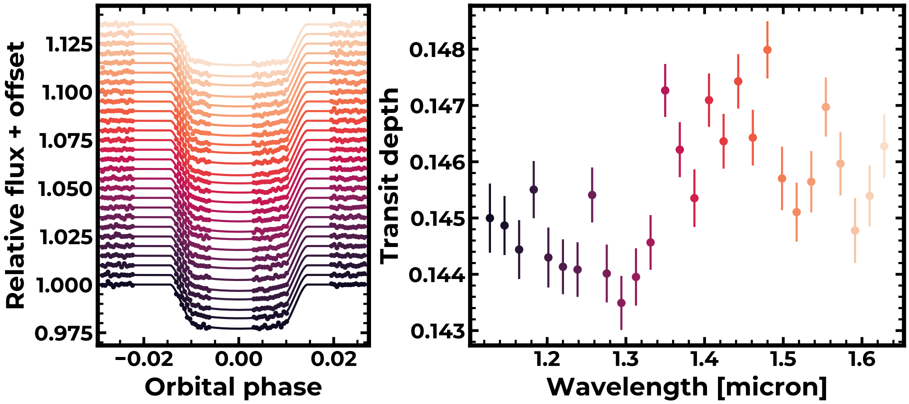

Figure 3.1: Transit light curves (left) of the hot Jupiter WASP-39 b, measured at near-infrared wavelengths, and the corresponding transmission spectrum (right), taken using the Wide Field Camera 3 on the Hubble Space Telescope (Wakeford et al. 2018). Courtesy of Hannah Wakeford.

From space-based observatories, these measurements yield spectroscopic light curves similar to Figure 3.1, since the light emitted from the star reaches the telescope without interacting with our own atmosphere. However, ground-based observations must contend with additional challenges, such as for example contamination from Earth's atmosphere, necessitating sophisticated techniques to isolate the planetary signal.

In recent years, high-resolution spectroscopy (HRS) has emerged as a powerful tool for characterising exoplanetary atmospheres from the ground (see Birkby 2018, for a review). By observing a star-planet system throughout parts of the planet's orbit, the relative orbital motion of the planet compared to the star and other contaminants enables the isolation of the planetary signal, see Figure 3.2. While HRS does not require the planet to transit its star (e.g. Brogi et al. 2012; Finnerty et al. 2024), this thesis focuses exclusively on transiting systems. This chapter first introduces the key method for studying transiting systems from the ground – high-resolution transmission spectroscopy – before detailing the observational requirements and challenges.

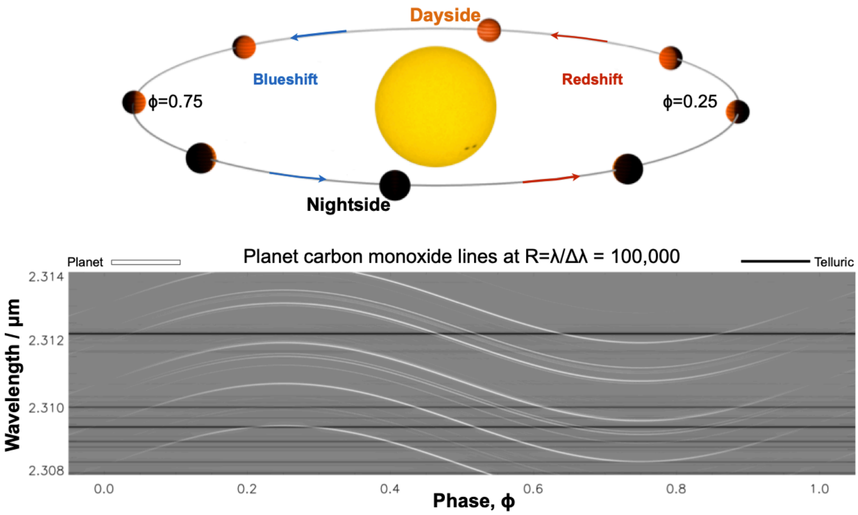

Figure 3.2: The high-resolution spectroscopy technique. The top panel shows the illumination of a non-transiting planet throughout its orbit and highlights when its spectrum is red- or blue-shifting. At high resolution, the planet's spectrum is resolved into a dense forest of individual lines in a pattern unique to each element in the planetary atmosphere. These lines trace out the radial velocity curve of the planet, allowing it to be robustly disentangled from the essentially stationary stellar lines and the contaminating spectral lines from Earth's telluric features. Figure reproduced from Birkby (2018) with permission.

3.1 High-resolution transmission spectroscopy

High-resolution transmission spectroscopy draws upon two key exoplanet detection techniques: the radial velocity method and the transit method. During the transit, a fraction of the starlight passes through the planet's upper atmospheric layers, resulting in the planet's spectral lines being superimposed on the star's, following

$$F_{\text{observed}}(\lambda) = F_*(\lambda)T(\lambda) = F_*(\lambda)\left(1 - \delta(\lambda)\right), \tag{3.1}$$

where F_* is the flux of the star, T is the effective transmission function of the planetary atmosphere, and $\delta(\lambda) = (R_{\text{p}}(\lambda)/R_*)^2$ is the wavelength-dependent transit depth[1].

Because the planet and star orbit their common centre of mass, the spectral lines from their respective atmospheres are Doppler-shifted to different radial velocities, and therefore wavelengths. Specifically, as the planet moves toward the observer, its spectral lines are blue-shifted, while the star's lines are redshifted due to its motion in the opposite direction. This relative motion results in a measurable Doppler shift that follows the relation (derived from the lever law)

$$v_{\text{RV},*} = -\frac{M_p}{M_*} v_{\text{RV,p}}, \tag{3.2}$$

where $v_{\text{RV},*}$ is the radial velocity of the star, also called the stellar reflex motion, $v_{\text{RV,p}}$ is the radial velocity of the planet, and M_p and M_* are the masses of the planet and star, respectively.

Given that $M_* \gg M_p$, the radial velocity of the star is several orders of magnitude smaller than that of the planet, thus the stellar lines appear approximately stationary, facilitating removal techniques to isolate the planetary spectrum.

For a circular orbit ($\varepsilon = 0$), the stellar reflex motion can be described by a simplified version of Equation (1.1):

$$v_{\text{RV},\star} = -K_* \sin(2\pi\phi), \tag{3.3}$$

where K_* is the stellar radial velocity semi-amplitude and $\phi = \frac{2\pi a}{P} = \frac{\theta(t)}{2\pi}$ (from Kepler's third law) is the orbital phase where $\phi = 0$ is the transit centre. In the case of eccentric orbits ($\varepsilon \neq 0$, as discussed in Paper IV), the stellar reflex motion depends on more parameters, namely, the orbital period P, the orbital eccentricity

[1] Note the difference compared to Equation (1.3).

ε, the time and argument of periastron $T_{\rm per}$ and ω, the mass of the star $M_\star$, the semi-major axis a, and the minimum mass of the planet $M_p \sin i$, where i is the orbital inclination. Note that circular orbits are defined to have $\omega := 90$ deg, such that $T_{\rm per} = T_0$, where T_0 is the transit centre time.

The true anomaly θ for eccentric orbits in Equation (1.1), unlike for circular orbits, cannot be solved analytically due to the lack of an analytical solution to Kepler's equation:

$$M = E - \varepsilon \sin E, \tag{3.4}$$

where M is the mean anomaly, ε is the eccentricity, and E is the eccentric anomaly. The true anomaly θ is then related to the eccentric anomaly E via:

$$\tan \frac{\theta}{2} = \sqrt{\frac{1+\varepsilon}{1-\varepsilon}} \tan \frac{E}{2}. \tag{3.5}$$

Hence, the stellar reflex motion $v_{\rm RV,\star}$ for eccentric orbits in Equation (1.1) can also only be computed numerically due to its dependence on the true anomaly θ, e.g., through `PyAstronomy`'s `KeplerRVmodel` (Czesla et al. 2019).

Observations from the ground are taken in the rest frame of the observatory on Earth. As Earth also moves around the common centre of mass of the Solar System, and rotates around its own axis, this introduces another velocity component crucial for the success of this technique: the barycentre velocity $v_{\rm berv}$.

To remove the stellar component, the observed spectra must be converted to the star's rest frame. This requires correcting the wavelengths for the barycentric velocity, stellar reflex motion, and systemic velocity using the relativistic longitudinal Doppler effect.:

$$\lambda_{\rm emitted} = \lambda_{\rm observed} \sqrt{\frac{1 + v_{\rm corr}/c}{1 - v_{\rm corr}/c}} \approx \lambda_{\rm observed} \left(1 + \frac{v_{\rm corr}}{c}\right), \tag{3.6}$$

where $\lambda_{\rm emitted}$ is the wavelength emitted at the source (i.e. the star), $\lambda_{\rm observed}$ is the wavelength observed at the telescope, c is the speed of light, and $v_{\rm corr}$ is given as

$$v_{\rm corr} = v_{\rm berv} - v_{\rm RV,\star} - v_{\rm sys}. \tag{3.7}$$

Note that the barycentre velocity has the opposite sign, provided these measurements are relative to the barycentre rest frame, not Earth.

While the barycentric and reflex motions vary with orbital phase, the systemic velocity correction is a constant offset. This correction is not strictly necessary for detecting atmospheric species, as their spectral signature is only shifted by the systemic velocity. However, applying the correction aids analysis, as signals centred on 0 velocity are easier to interpret.

3.2 Observing planetary atmospheres

Knowing that planetary and stellar lines shift relative to each other, it should in principle be relatively straightforward to extract the atmosphere of an exoplanet from observations. However, optimising the science yield when observing these systems requires a careful strategy. This section provides a brief overview of key considerations for observation planning and the contamination sources that complicate the isolation of the planetary signal.

3.2.1 Strategy

During a planetary transit, the telescope is pointed at the host star, collecting light that has passed through the planetary atmosphere. Rather than capturing all the light in a single long exposure (i.e., integrating over the entire transit duration), the observations are divided into shorter exposures. This strategy helps isolate the planetary signal from various sources of contamination as it moves significantly between each exposure, and avoids saturation in the case of bright systems. The signal-to-noise ratio (S/N) is the critical quantity every observer seeks to optimise without compromising the necessary level of detail linked to the planetary atmosphere. The S/N (in the photon-noise limited regime) of the planet is linked to that of the star via

$$\mathrm{SNR}_{\mathrm{planet}} = \left(\frac{F_p}{F_*}\right) \mathrm{SNR}_*, \tag{3.8}$$

where $\mathrm{SNR}_{\mathrm{planet}}$ and F_p, and SNR_* and F_* are the S/N and flux of the planet and star, respectively. Thus, to maximise the S/N of the planet, it would be favourable to maximise the S/N of the star. However, this entails observing as long as possible on the source (before saturating the detector), which in turn would hinder the isolation of the planetary signal from that of the star and other contamination sources. Therefore, optimising exoplanetary transit observations essentially hinges on one key parameter: the exposure time (Boldt-Christmas et al. 2024).

Exposure time refers to the duration spent collecting light from a system before the detector is read out and a new round of collection is initiated. If the exposure time is too short, too few photons are collected, leading to a low S/N that may hinder the scientific case. Conversely, excessively long exposures introduce an effect known as smearing, where the planet's motion during integration blurs the otherwise narrow absorption lines in its atmosphere, causing them to appear broadened. These competing effects are especially critical when observing relatively faint systems with short-period planets, where longer exposures are required to obtain sufficient S/N. However, for systems with bright host stars, this trade-off is less problematic. A bright star allows for short exposure times that achieve both high S/N and minimal smearing. An example of such a system is the fast-rotating A-type star WASP-189 and its ultra-hot Jupiter companion, WASP-189 b, the focus of Papers I–III.

3.2.2 Contamination sources

As light from the system travels toward the observer, it first traverses the interstellar medium (ISM) and then Earth's atmosphere. Along this path, these sources of contamination imprint additional features onto the observed spectra.

The dominant source of contamination is the Earth's atmosphere. Telluric absorption, particularly strong in the infrared, is primarily caused by water vapour (H_2O) and hydroxide (OH), which significantly affects observations. While weaker in the optical regime, telluric contamination remains relevant due to absorption by water vapour and molecular oxygen (O_2), most notably near 760 nm and 690 nm, respectively. In addition to absorption, telluric emission from the Earth's atmosphere, arising from species such as sodium, ferrous oxide (FeO), OH, and O_2, can introduce further contamination, particularly in the near-infrared through nightglow (Biondi & Feibelman 1968; Bates 1988; Cosby et al. 2006; Saran et al. 2011). However, both telluric absorption and emission are fixed in the observatory's rest frame, making it possible to schedule observations such that these contaminating features shift away from the planetary rest frame. This shift is governed by Earth's barycentric velocity around the solar system's centre of mass (see Section 3.3.1).

Another potential source of contamination is absorption by sodium in the ISM, depending on the location of the observed system within the galaxy (Heger 1919). This contamination can be readily identified through visual inspection, as it appears as nearly saturated absorption features (see Figure 3.3). When present, these features can be effectively mitigated by masking the affected spectral regions.

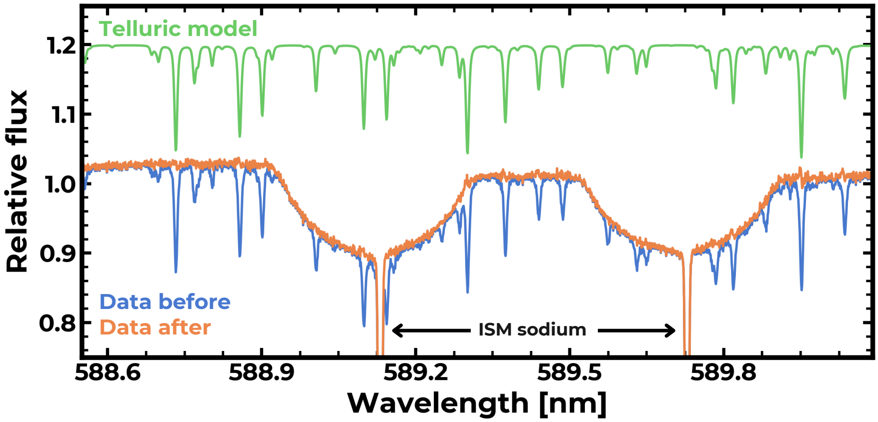

Figure 3.3: Correction of telluric absorption by H_2O around the Na D lines. The best-fit model (in green) was computed with `molecfit` (Kausch et al. 2015; Smette et al. 2015). The data before and after telluric correction are shown in blue and orange respectively. The contamination through the sodium lines of the interstellar medium are indicated in the figure.

3.2.3 Rossiter-McLaughlin effect

During transit, a planet sequentially obscures different regions of the rotating stellar disc, inducing an apparent radial velocity anomaly in spectral lines. This phenomenon, first described by Rossiter (1924) and McLaughlin (1924), is now known as the Rossiter-McLaughlin (RM) effect. For an aligned orbit, the planet initially covers the approaching (blue-shifted) regions before moving across to block the receding (red-shifted) regions, distorting the stellar line profiles. The shape and amplitude of this effect depend on the planet's trajectory and its alignment with the stellar rotation axis. Figure 3.4 illustrates how variations in spin-orbit alignment produce distinct RM signatures.

In exoplanet spectroscopy, this stellar obscuration during transit introduces residual spectral features when performing differential transmission spectroscopy where spectra are divided to isolate the planetary signal. These residual lines appear at the velocity of the blocked stellar regions and can overlap with planetary absorption features, complicating their extraction (e.g. Casasayas-Barris et al. 2022).

The affected velocities are dictated by the planet's position along its orbit and the star's projected rotational velocity, and are given by

$$v_{\rm RM} = v \sin I_* [x_{\rm op}(-\cos\lambda \cos\omega + \sin\lambda \cos i \sin\omega) \tag{3.9}$$

$$+ y_{\rm op}(\cos\lambda \sin\omega + \sin\lambda \cos i \cos\omega)], \tag{3.10}$$

where $v \sin I_*$ is the projected rotational velocity of the star, λ is the projected orbital obliquity, ω is the argument of periastron and i is the inclination of the orbit with respect to the plane of the sky ($i \approx 90$ deg for transiting systems).

The coordinates of the planet in the orbital plane of the sky, $x_{\rm op}$ and $y_{\rm op}$, are given by

$$x_{\rm op} = \frac{a}{R_*}\left(\cos E - \varepsilon\right), \quad y_{\rm op} = \frac{a}{R_*}\sqrt{1-\varepsilon^2}\sin E, \tag{3.11}$$

for eccentric orbits, and by

$$x_{\rm op} = \frac{a}{R_*}\cos(2\pi\phi), \quad y_{\rm op} = \frac{a}{R_*}\sin(2\pi\phi), \tag{3.12}$$

for circular orbits. $\frac{a}{R_*}$ is the scaled semi-major axis, E is the eccentric anomaly, ε is the eccentricity and ϕ is the orbital phase (only valid for $\varepsilon = 0$). A full derivation of Equation (3.10) is provided in Paper IV.

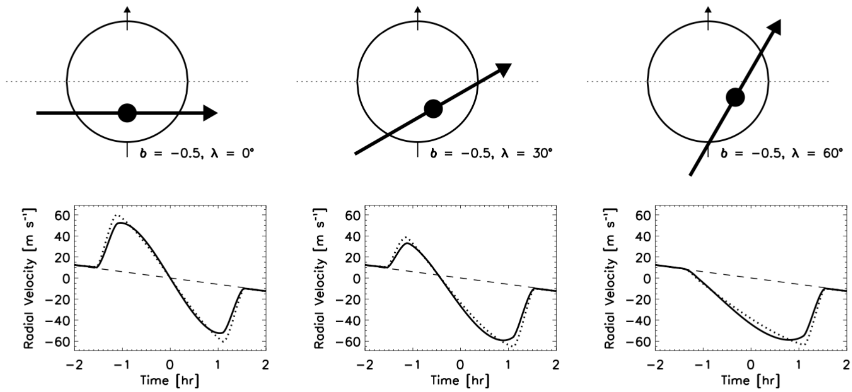

Figure 3.4: Rossiter-McLaughlin effect for various orbital configurations. *Top panels:* Orbital configurations. The projected orbital obliquity λ determines the alignment of the planetary orbit with respect to the stellar rotation axis. The impact parameter is given as $b = \frac{a}{R_*} \cos i$, where a is the semi-major axis, R_* is the stellar radius and i is the inclination of the orbit. See Figure 1.2 for orbital elements. *Bottom panels:* Observed RM effect for the given orbital configuration as radial velocity deviation as a function of time. Figure from Gaudi & Winn (2007). ©AAS. Reproduced with permission.

3.3 Limitations

Observing from the ground inherently involves certain limitations, which become more pronounced for planets with longer orbital periods. As the orbital velocity of these planets decreases, the ability to isolate the subtle signals is further constrained by the aforementioned contamination sources: the star, the RM effect, and tellurics. The successful isolation of the planetary signature therefore hinges on the *need for speed* and careful scheduling.

3.3.1 The need for speed

A planet must undergo a sufficiently large radial velocity change during transit to distinguish its atmospheric signal from stellar and telluric contamination. This velocity shift, computed using Equation (4.3), depends on well-constrained orbital parameters. When combined with Equation (3.10) and Equation (1.1), all velocity components in the system can be determined. This is a challenge particularly for cooler planets on longer orbits, with slower orbital velocities and extended transit durations. Without a sufficiently large velocity shift, the planetary signal remains blended with the contamination sources, limiting its detectability. Figure 3.5 illustrates these velocity traces for three planets with distinct orbital properties.

The ultra-hot Jupiter WASP-189 b provides a clear example of favourable conditions for atmospheric characterisation. It orbits its host star every three days on a nearly polar orbit and experiences a substantial radial velocity change of $80\,\mathrm{km\,s^{-1}}$ during transit, ranging from $-40\,\mathrm{km\,s^{-1}}$ at ingress to $40\,\mathrm{km\,s^{-1}}$ at egress.

In contrast, WASP-130 b, a warm gas giant on a circular, aligned, approximately 10-day orbit, exhibits a far smaller velocity shift, increasing from $3\,\mathrm{km\,s^{-1}}$ at ingress to $9.5\,\mathrm{km\,s^{-1}}$ at egress, resulting in a total change of just $6.5\,\mathrm{km\,s^{-1}}$. Given a typical exposure time of 300 s, the planet moves by only $200\,\mathrm{m\,s^{-1}}$, which is well below the resolving power of current high-resolution spectrographs (e.g. ESPRESSO: $v_{\mathrm{res,HR}} \approx 500\,\mathrm{m\,s^{-1}}$). As a result, its atmospheric signal remains indistinguishable from the star and RM effect, which appear nearly stationary in comparison.

Finally, TOI-3362 b, a warm gas giant on a highly eccentric orbit, presents a more favourable case for detection. Despite having an orbital period comparable to WASP-130 b, its high eccentricity ($\varepsilon = 0.7$) and argument of periastron ($\omega = 60$ deg) result in a significant velocity shift during transit.

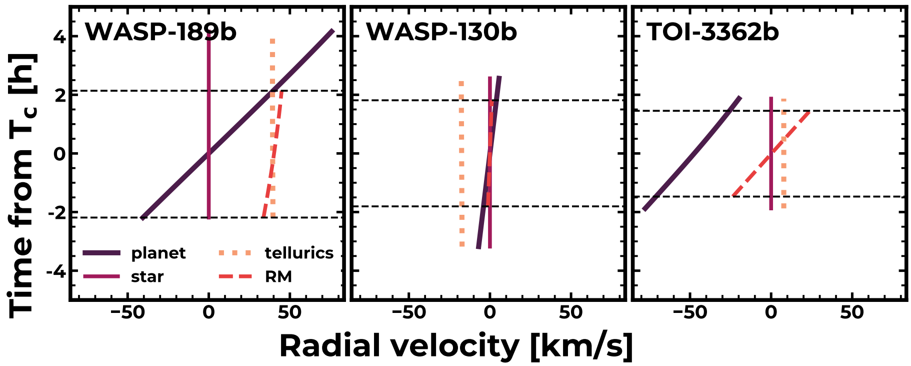

Figure 3.5: Radial velocity traces of WASP-189 b (left), WASP-130 b (middle), and TOI-3362 b computed with the `RVTraceEstimator` published as part of Paper IV. Radial velocities of the planet (dark purple, solid), star (pink, solid), RM effect (red, dashed) and telluric contamination (light orange, dotted) are given in the rest frame of the system. The dashed black lines indicate the transit contact times. WASP-189 b and WASP-130 b reside on circular orbits, while TOI-3362 b's orbit has an eccentricity of $\varepsilon = 0.7$.

3.3.2 Telluric contamination and observation planning

Careful planning of observation windows is crucial to minimising telluric contamination, particularly for planets with strong infrared absorption bands, such as H_2O and CO. Since Earth's barycentric motion dictates the rest frame of these telluric features, scheduling observations accordingly can improve signal isolation.

While this optimisation is less critical for fast-orbiting planets, it becomes increasingly important for those with longer periods, where lower orbital velocities make detecting subtle atmospheric signals more challenging. Overlapping absorption by H_2O and CO in Earth's atmosphere can interfere with planetary features, but strategic timing can help mitigate this effect.

Chapter 4

Atmospheric detection

"We have peered into a new world, and have seen that it is more mysterious and more complex than we had imagined. Still, the quest continues."

– Vera Rubin

It is perhaps unsurprising that, following the first detection of an exoplanetary atmosphere with the Space Telescope Imaging Spectrograph aboard the Hubble Space Telescope (Charbonneau et al. 2002), attempts were made to confirm this detection from the ground (e.g. Narita et al. 2005). Sodium absorption was later confirmed (Snellen et al. 2008) in HD 209458 b, and was also detected in another short-period, hot Jupiter-like planet, HD189733 b (Redfield et al. 2008).

These early observations were crucial in advancing ground-based studies of exoplanetary atmospheres, as they demonstrated the feasibility of overcoming the challenges posed by Earth's atmosphere. As shown in Figure 3.3, the sodium doublet falls within a telluric water band, making these detections a significant step toward mitigating telluric contamination and enabling more robust atmospheric characterisation.

However, while these observations detected a flux change during transit in the sodium doublet, they did not resolve the planet's sodium feature. Instead, the observed flux variation was attributed to absorption by the planetary atmosphere. The absorption lines from the planet are much shallower than those from its host star, remaining *hidden in the noise*, and therefore undetectable by eye in the observed spectrum. As discussed in Chapter 3, the planet's S/N depends on the flux ratio between the planet and its star, with the stellar contribution dominating the spectrum.

To address this challenge, several techniques have been developed to enhance the planetary signal. The two most prominent methods, both relying on large velocity shifts during transit – the need for speed discussed in Chapter 3 – are introduced in this chapter.

4.1 Cross-correlation technique

It is generally not possible to visually identify the absorption lines of the planet in a single exposure, as the star dominates the observed spectrum. Even if the stellar component were perfectly removed, the absorption lines of the planet would often remain below the noise level.

To mitigate this, one can leverage the entire wavelength range of the spectrograph used for the observation. Instead of searching for a single absorption line of the planet, the contributions of all absorption lines within the spectrograph's wavelength range for a given chemical species (i.e., atom or molecule) can be averaged, a method termed the cross-correlation technique.

At the core of this technique lies the cross-correlation function, which quantifies the degree of correlation between observed spectra and a template spectrum. Given an observed spectrum $F_i(\lambda, t)$ at time t, the cross-correlation function $C(v, t)$ is computed as

$$C(v,t) = \sum_{i=0}^{N} F_i(\lambda, t) T_i(v), \tag{4.1}$$

where $T(v)$ represents the cross-correlation template shifted to a radial velocity v and is normalised such that $\sum_{i=0}^{N} T_i(v) = 1$.

Figure 4.1 illustrates how the cross-correlation function is obtained for a single spectrum in the time series. The cross-correlation coefficients are then computed for each exposure using the transmission spectrum of a given species as the model template T in Equation (4.1). This procedure produces a two-dimensional cross-correlation function for each time series and each species. The associated uncertainties are, or can generally be determined via Gaussian error propagation of the expected photon noise.

By cross-correlating all available absorption lines of a given atmospheric species, the planet's S/N (see Equation 3.8) can be enhanced by approximately a factor of $\sqrt{N_{\text{lines}}}$, where N_{lines} is the number of detected lines in the spectrum. Since some species exhibit hundreds or even thousands of absorption lines, this technique can improve the S/N by a factor of 10–30.

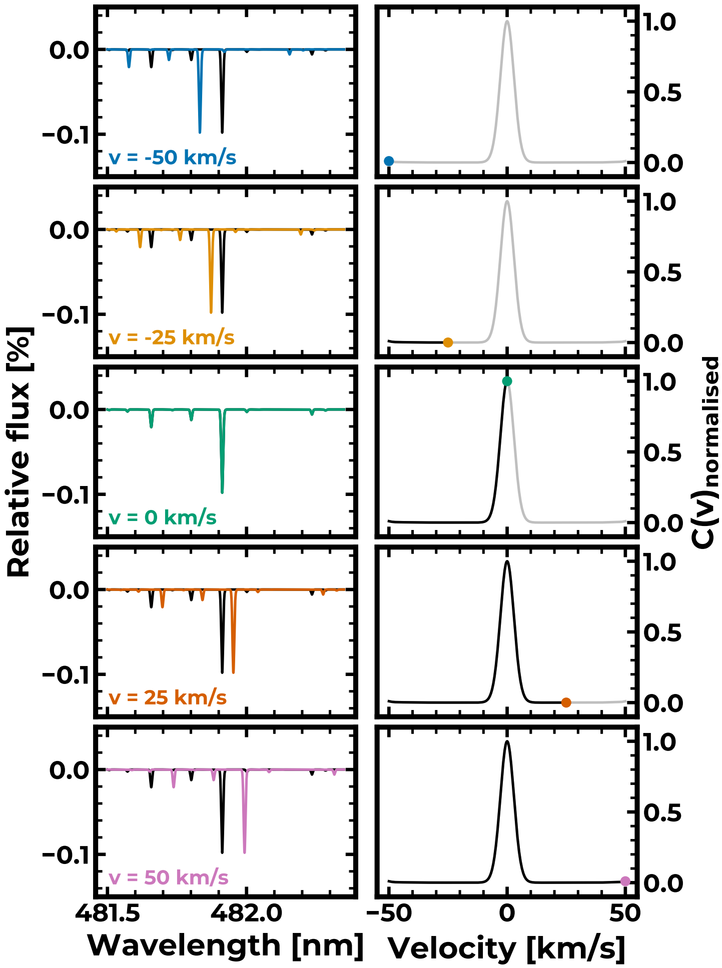

Figure 4.1: Illustration of the cross-correlation technique. *Left*: Observed flux (black) overlaid with a shifted template (coloured) for a given velocity. *Right*: The renormalised cross-correlation function, $C_{\text{normalised}}(v)$, showing the template's contribution at different velocities. An animated version is available at CCF visualisation.

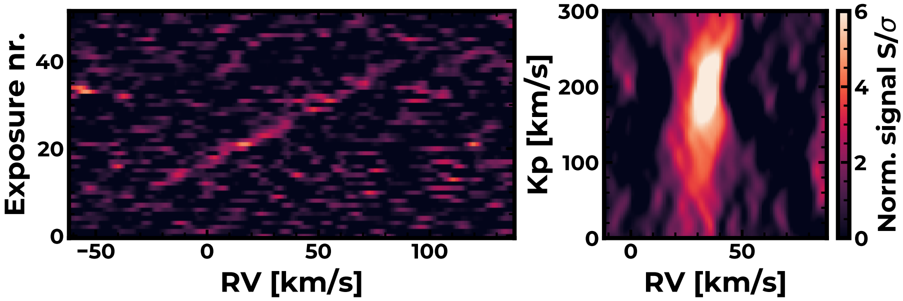

Figure 4.2: Cross-correlation detection of Ti in WASP-121 b with data from Prinoth et al. (2025). The left panel shows the two-dimensional cross-correlation function. The planetary atmosphere is shown as a bright slanted feature. The right panel shows the K_p–v_{sys} map. Note that the two panels are on the same colour scale to showcase the improvement in S/N.

However, the S/N may still be too low, resulting in the two-dimensional cross-correlation function not immediately revealing a detected species (e.g., titanium oxide in Paper I). To further enhance the S/N, the spectra can be shifted into the planetary rest frame by applying the (additional) velocity correction v_{corr}:

$$v_{\text{corr}} = v_{\text{RV},*} - v_{\text{RV,p}}, \tag{4.2}$$

where $v_{\text{RV},*}$ is the radial velocity of the star, and $v_{\text{RV,p}}$ is the planet's radial velocity, determined by:

$$v_{\text{RV,p}} = K_p \left[\cos\left(\theta + \omega\right) + \varepsilon \cos\left(\omega\right)\right]. \tag{4.3}$$

As the projected orbital velocity K_p may not be known a priori since it depends on the orbital inclination i, one can scan through different K_p values instead of assuming a single value (Brogi et al. 2012). For each K_p, the shifted exposures are averaged in time, enhancing the S/N by a factor of $\sqrt{N_{\text{exp}}}$ and aiding the detection of species that may be difficult to identify in the original cross-correlation function. Figure 4.2 shows the detection of Ti in two different representations, highlighting the improvement in S/N through stacking in the planetary rest frame.

The cross-correlation technique, originally developed for stars and galaxies by Simkin (1974), was first successfully applied to exoplanets in 2010 with the detection of carbon monoxide in HD 209458 b using the CRIRES spectrograph (Snellen et al. 2010). This demonstrated the potential of high-resolution spectroscopy to detect molecular species. Since then, the technique has been used to detect a variety of species, including water, and has been instrumental in revealing atmospheric compositions of exoplanets (e.g. Brogi et al. 2012; Birkby et al. 2013; Snellen et al. 2014, for early successes).

A significant milestone came in 2018 with the detection of atomic metal absorption in the ultra-hot Jupiter KELT-9 b, which underscored the extreme conditions of such planets and highlighted the ability of cross-correlation to detect atomic and ionised species (Hoeijmakers et al. 2018, 2019). Since then, the cross-correlation technique has become a standard tool for detecting atomic and ionised species (e.g. Pino et al. 2020; Gibson et al. 2020; Hoeijmakers et al. 2020; Borsa et al. 2021; Sedaghati et al. 2021; Merritt et al. 2021; Gibson et al. 2022; Pino et al. 2022; Gandhi et al. 2022; Borsato et al. 2023; Pelletier et al. 2023; Maguire et al. 2023; Hoeijmakers et al. 2024; Silva et al. 2024, to name just a few). Among these, WASP-121 b, WASP-76 b, and WASP-189 b have become benchmark targets for atmospheric studies, boasting extensive inventories of detected species and detailed phase-resolved observations (e.g. Ehrenreich et al. 2020; Borsa et al. 2021; Wardenier et al. 2024; Hoeijmakers et al. 2024; Prinoth et al. 2025).

4.2 Narrow-band transmission spectroscopy

Complementary to the cross-correlation technique, narrow-band transmission spectroscopy emerged as a tool to investigate the uppermost layers of the atmosphere of hot exoplanets. While cross-correlation exploits thousands of absorption lines from atomic or molecular species, narrow-band spectroscopy focuses on specific, deep absorption features.

This technique builds on the principles of differential transmission spectroscopy (Wyttenbach et al. 2015), first used to confirm the presence of sodium in HD 189733 b from the ground. By comparing the system's flux during transit, $F_{\mathrm{i,in}}$ (where i indicates the exposure number), with the flux outside of transit, $F_{\mathrm{i,out}}$, the transmission spectrum is constructed as their ratio. This reveals atmospheric contributions that are not associated with the stellar spectrum.

The transmission spectrum as a function of wavelength, λ, in the stellar rest frame is given by

$$T_i(\lambda) = \frac{F_{\mathrm{i,in}}(\lambda)}{\sum_i F_{\mathrm{i,out}}(\lambda)} = \frac{F_{\mathrm{i,in}}(\lambda)}{F_{\mathrm{out}}(\lambda)}, \tag{4.4}$$

where $F_{\mathrm{out}}(\lambda)$ is the sum of all out-of-transit exposures (Charbonneau et al. 2002; Redfield et al. 2008). This approach effectively removes the stellar contribution, assuming that the star's flux remains relatively constant over the duration of the transit.

In most cases, the planetary signal may not be resolved in phase due to insufficient S/N. To enhance the S/N, the transmission spectra are shifted into the planetary rest frame using Equation (3.7) and then averaged over time.

Since the detection of sodium (Wyttenbach et al. 2015), narrow-band transmission spectroscopy has proven to be a powerful tool for detecting a variety of species in exoplanetary atmospheres. Key examples in the optical and near-infrared regions include the detection of Na Fraunhofer D-lines (e.g. Wyttenbach et al. 2015; Seidel et al. 2019), the hydrogen Balmer series and Lyman-α line (e.g. Lecavelier Des Etangs et al. 2010; Bourrier et al. 2013; Ehrenreich et al. 2015; Wyttenbach et al. 2020), K and Li (e.g. Sing et al. 2011; Sedaghati et al. 2016; Chen et al. 2020, 2022), the He line at 1.0833 nm (e.g. Allart et al. 2018; Nortmann et al. 2018; Czesla et al. 2022), and the Ca^+ infrared triplet (e.g. Langeveld et al. 2025). Only very recently, improvements in observation quality, mainly driven by the use of stable spectrographs mounted on large telescopes that allow high S/N observations, have made it possible to detect planetary signatures without time-averaging for some of the hottest and brightest targets (see e.g. Simonnin et al. 2024; Langeveld et al. 2025), as also demonstrated in Paper III of this thesis.

Unlike the cross-correlation technique, the detection of individual resolved lines does not rely on template models and is therefore not inherently dependent on assumptions about the atmosphere's chemical composition. When combined with dynamics retrievals, this method becomes a powerful tool for measuring atmospheric winds, including day-to-night-side flows, and equatorial jets (Seidel et al. 2020, 2021, 2023, 2025).

4.3 Noteworthy challenges

The Ti detection in Figure 4.2 highlights the remarkable progress of the cross-correlation technique – and the field as a whole – over the past decade and a half. From early struggles with telluric contamination to resolving atmospheric signals in time, these advancements have enabled the detection of species once thought to be depleted or even absent from exoplanetary atmospheres. A striking example is the detection of Ti in WASP-121 b, a planet that straddles critical temperature regimes where Ti-bearing species may condense and rain out, and were previously thought to do so (e.g. Hoeijmakers et al. 2020; Gandhi et al. 2023; Maguire et al. 2023; Hoeijmakers et al. 2024; Pelletier et al. 2024; Prinoth et al. 2025). The presence of Ti in transmission – detected thanks to higher S/N observations – suggests complex vertical and horizontal transport processes, underscoring the need for refined models of atmospheric chemistry and dynamics (Prinoth et al. 2025).

Given the presence of Ti in WASP-121 b, TiO is expected to be present as well, yet it has remained elusive. This persistent non-detection likely stems from a combination of factors, such as limitations in line lists (Hoeijmakers et al. 2015; McKemmish et al. 2019) and the difficulty of extracting a weak signal from observational noise (Prinoth et al. 2025). This challenge extends beyond WASP-121 b, as efforts to confirm TiO in ultra-hot Jupiter atmospheres have often resembled a game of *effeuiller la marguerite*[1], with detections reported in both low- and high-resolution observations (e.g. Nugroho et al. 2017; Sedaghati et al. 2017), only to be contradicted by follow-up studies (e.g. Herman et al. 2020; Serindag et al. 2021; Espinoza et al. 2019; Sedaghati et al. 2021). Papers I and II of this thesis contribute to resolving this debate for WASP-189 b by presenting the first confirmed ground-based detection of TiO in an exoplanetary atmosphere via transmission spectroscopy. Future facilities such as the Extremely Large Telescope (ELT) will be crucial in pushing beyond current limitations in S/N and spectral coverage, providing a definitive answer on the presence of TiO in WASP-121 b and similar planets.

[1] An originally French game most of us probably know as "love me, love me not".

Chapter 5

Conclusion and outlook

"Why do we study the universe? Why do we look at the sky and ask questions, build telescopes, travel to the very limits of our planet to answer them? Why do we stargaze?

We don't know exactly why, but we must."

– Emily M. Levesque, *The Last Stargazers*

The field of exoplanetary science is relatively young, yet it has advanced in giant leaps: from the first detection of planets outside our solar system (Campbell et al. 1988) to the study of layered wind patterns in exoplanetary atmospheres (Seidel et al. 2025) in less than forty years. Some of these atmospheric observations were anticipated by theory, such as the role of titanium and vanadium oxides, which continue to present challenges. Others have expanded our understanding, revealing phenomena such as two-peaked jets (Nortmann et al. 2025) or prompting us to reconsider expected vertical structures in exoplanetary atmospheres (Seidel et al. 2025).

The work presented in this thesis has contributed to several key developments in this field. Paper I presents the first detection of TiO in the transmission of an ultra-hot Jupiter at high spectral resolution, a result that is confirmed and further explored in Paper II. These follow-up observations also reveal a range of strong absorption features, leading to phase-resolved detections using the cross-correlation technique (Paper II) and even detections of individual lines (Paper III). Paper III serves as a spectral atlas, providing a robust benchmark for testing atmospheric models. Lastly, Paper IV pushes the boundaries of what is achievable with current instruments and methods for cooler planets, paving the way for upcoming facilities and challenging existing approaches.

As we enter an era of increasingly powerful instrumentation, the study of exoplanetary atmospheres is on the brink of a revolution. Both ground- and space-based observatories are poised to provide unprecedented insights into these distant worlds. The following sections highlight some of the most exciting prospects, without aiming to provide an exhaustive or definitive account.

High-resolution spectroscopy in the ELT era. One of the most promising developments for the field is the construction of ESO's Extremely Large Telescope (ELT), expected to achieve first light by the end of this decade. With its 39-meter primary mirror, the ELT will dramatically enhance our ability to observe exoplanetary atmospheres at high spectral resolution.

Among the ELT's extensive suite of instruments, the ArmazoNes high Dispersion Echelle Spectrograph (ANDES) stands out as particularly promising for exoplanetary science (Marconi et al. 2024). As a second-generation instrument, ANDES will offer a resolving power comparable to existing high-resolution spectrographs, but with improved sensitivity, thanks to the ELT's vast collecting area. This will enable the resolution of individual absorption lines with unprecedented detail, facilitating precise measurements of atmospheric composition, temperature, and dynamics (Palle et al. 2023). Complementary instruments, such as the High Angular Resolution Monolithic Optical and Near-infrared Integral field spectrograph (HARMONI), the Mid-infrared ELT Imager and Spectrograph (METIS), or the Planetary Camera and Spectrograph (PCS), will further extend our capacity for atmospheric characterisation by offering medium- to high-resolution spectroscopy through integral field units (Houllé et al. 2021; Kasper et al. 2021; Brandl et al. 2021).

Regardless of the specific instrument used, the ELT is expected to bring breakthroughs not only for the study of hot and warm gas giants but also for their cooler, less-irradiated counterparts.

Synergies between ground- and space-based observations. In the coming years, we will witness not only advancements in ground-based capabilities but also significant contributions from space-based observatories. The JWST has already begun to deliver results (e.g. Rustamkulov et al. 2023; Ahrer et al. 2023; Feinstein et al. 2023, for early results), and future missions, such as the Atmospheric Remote-sensing Infrared Exoplanet Large Survey (ARIEL) and the proposed Habitable Worlds Observatory (HWO), are set to continue providing valuable insights into exoplanetary atmospheres (e.g. Tinetti et al. 2018; Harada et al.

2024). These missions excel at measuring the band heads of molecular features, complementing the high-resolution observations achievable from the ground.

By leveraging synergies across multiple telescopes and observational techniques, we will be able to combine their respective strengths and work towards a more complete understanding of exoplanetary atmospheres (e.g. Brogi et al. 2017; Brogi & Line 2019; Pino et al. 2018). This will allow for probing different atmospheric layers and assessing the vertical distribution of chemical species (e.g. Smith et al. 2024).

This multi-instrument approach will be essential for building a comprehensive understanding of exoplanetary atmospheres, bridging the gap between observational techniques and theoretical models.

Connecting atmospheric observations to planet formation. One of the ultimate goals of atmospheric studies is to establish a connection between present-day atmospheric properties and the formation and evolution of exoplanetary systems (e.g. Öberg et al. 2011; Madhusudhan et al. 2014). By measuring elemental abundances such as CO or refractories / volatiles, we can begin to infer the formation environments of these planets and their subsequent migration histories (e.g. Lothringer et al. 2021; Pelletier et al. 2023, 2024; Coria et al. 2024; Lothringer et al. 2025).

In summary, the future of exoplanetary science is incredibly exciting, fuelled by cutting-edge observational advancements and the growing synergy between ground- and space-based observatories. While challenges remain – the complexities of interpreting observations, overcoming instrument limitations, addressing stellar activity, and ensuring long-term mission sustainability – the field is poised for growth. Exoplanetary science will continue to be deeply intertwined with other fields, and as we refine our techniques and deepen our understanding, we will not only gain new insights into exoplanetary atmospheres but also uncover clues about the formation and evolution of planetary systems, including our own. Current observations are pushing the limits of what is possible, and the future is definitely bright.

Bibliography

Adams, W. S., & Dunham, Jr., T. 1932, Publications of the Astronomical Society of the Pacific, 44, 243, doi: 10.1086/124235

Adel, A., & Slipher, V. M. 1934, Physical Review, 46, 240, doi: 10.1103/PhysRev.46.240

Agol, E., Steffen, J., Sari, R., & Clarkson, W. 2005, MNRAS, 359, 567, doi: 10.1111/j.1365-2966.2005.08922.x

Ahrens, C. 1994, Meteorology today: An introduction to weather, climate, and the environment, 5th edn. (WEST PUBLISHING COMPANY, COLLEGE & SCHOOL DIVISION)

Ahrer, E.-M., Stevenson, K. B., Mansfield, M., et al. 2023, Nature, 614, 653, doi: 10.1038/s41586-022-05590-4

Allart, R., Bourrier, V., Lovis, C., et al. 2018, Science, 362, 1384, doi: 10.1126/science.aat5879

Arcangeli, J., Désert, J.-M., Line, M. R., et al. 2018, The Astrophysical Journal Letters, 855, L30, doi: 10.3847/2041-8213/aab272

Arras, P., & Socrates, A. 2010, The Astrophysical Journal, 714, 1, doi: 10.1088/0004-637X/714/1/1

Ballard, S., Fabrycky, D., Fressin, F., et al. 2011, The Astrophysical Journal, 743, 200, doi: 10.1088/0004-637X/743/2/200

Bates, D. R. 1988, Planetary and Space Science, 36, 875, doi: 10.1016/0032-0633(88)90093-1

Bell, K. L., & Berrington, K. A. 1987, Journal of Physics B Atomic Molecular Physics, 20, 801, doi: 10.1088/0022-3700/20/4/019

Bell, T. J., & Cowan, N. B. 2018, ApJL, 857, L20, doi: 10.3847/2041-8213/aabcc8

Biondi, M. A., & Feibelman, W. A. 1968, Planetary and Space Science, 16, 431, doi: 10.1016/0032-0633(68)90158-X

Birkby, J. L. 2018, Exoplanet Atmospheres at High Spectral Resolution, doi: 10.48550/arXiv.1806.04617

Birkby, J. L., de Kok, R. J., Brogi, M., et al. 2013, Monthly Notices of the Royal Astronomical Society, 436, L35, doi: 10.1093/mnrasl/slt107

Boldt-Christmas, L., Lesjak, F., Wehrhahn, A., et al. 2024, Astronomy and Astrophysics, 683, A244, doi: 10.1051/0004-6361/202347398

Bond, I. A., Udalski, A., Jaroszynski, M., et al. 2004, The Astrophysical Journal, 606, L155, doi: 10.1086/420928

Borsa, F., Allart, R., Casasayas-Barris, N., et al. 2021, Astronomy and Astrophysics, 645, A24, doi: 10.1051/0004-6361/202039344

Borsato, N. W., Hoeijmakers, H. J., Prinoth, B., et al. 2023, A&A, 673, A158, doi: 10.1051/0004-6361/202245121

Borucki, W. J., Koch, D., Basri, G., et al. 2010, Science, 327, 977, doi: 10.1126/science.1185402

Bourrier, V., Lecavelier des Etangs, A., Dupuy, H., et al. 2013, Astronomy and Astrophysics, 551, A63, doi: 10.1051/0004-6361/201220533

Brandl, B., Bettonvil, F., van Boekel, R., et al. 2021, METIS: The Mid-infrared ELT Imager and Spectrograph

Brogi, M., Line, M., Bean, J., Désert, J. M., & Schwarz, H. 2017, The Astrophysical Journal, 839, L2, doi: 10.3847/2041-8213/aa6933

Brogi, M., & Line, M. R. 2019, The Astronomical Journal, 157, 114, doi: 10.3847/1538-3881/aaffd3

Brogi, M., Snellen, I. A. G., de Kok, R. J., et al. 2012, Nature, 486, 502, doi: 10.1038/nature11161

Brown, T. M. 2001, The Astrophysical Journal, 553, 1006, doi: 10.1086/320950

Burrows, A., Budaj, J., & Hubeny, I. 2008, The Astrophysical Journal, 678, 1436, doi: 10.1086/533518

Campbell, B., Walker, G. A. H., & Yang, S. 1988, The Astrophysical Journal, 331, 902, doi: 10.1086/166608

Casasayas-Barris, N., Palle, E., Stangret, M., et al. 2021, Astronomy and Astrophysics, 647, A26, doi: 10.1051/0004-6361/202039539

Casasayas-Barris, N., Borsa, F., Palle, E., et al. 2022, A&A, 664, A121, doi: 10.1051/0004-6361/202143016

CCF visualisation. Accessed: March 24, 2025, https://bibianaprinoth.ch/images/ccf.gif

Charbonneau, D., Brown, T. M., Latham, D. W., & Mayor, M. 2000, The Astrophysical Journal, 529, L45, doi: 10.1086/312457

Charbonneau, D., Brown, T. M., Noyes, R. W., & Gilliland, R. L. 2002, The Astrophysical Journal, 568, 377, doi: 10.1086/338770

Chauvin, G., Lagrange, A.-M., Dumas, C., et al. 2004, Astronomy & Astrophysics, 425, L29, doi: 10.1051/0004-6361:200400056

—. 2005, Astronomy & Astrophysics, 438, L25, doi: 10.1051/0004-6361:200500116

Chauvin, G., Desidera, S., Lagrange, A.-M., et al. 2017, Astronomy & Astrophysics, 605, L9, doi: 10.1051/0004-6361/201731152

Chen, G., Casasayas-Barris, N., Pallé, E., et al. 2020, Astronomy & Astrophysics, 635, A171, doi: 10.1051/0004-6361/201936986

Chen, G., Wang, H., van Boekel, R., & Pallé, E. 2022, The Astronomical Journal, 164, 173, doi: 10.3847/1538-3881/ac8df6

Coria, D. R., Hejazi, N., Crossfield, I. J. M., & Rhem, M. 2024, The Astrophysical Journal, 974, 151, doi: 10.3847/1538-4357/ad7020

Cosby, P. C., Sharpee, B. D., Slanger, T. G., Huestis, D. L., & Hanuschik, R. W. 2006, Journal of Geophysical Research (Space Physics), 111, A12307, doi: 10.1029/2006JA012023

Currie, T., Biller, B., Lagrange, A., et al. 2023, 534, 799, doi: 10.48550/arXiv.2205.05696

Czesla, S., Schröter, S., Schneider, C. P., et al. 2019, PyA: Python astronomy-related packages

Czesla, S., Lampón, M., Sanz-Forcada, J., et al. 2022, Astronomy and Astrophysics, 657, A6, doi: 10.1051/0004-6361/202039919

DACE Opacity Database. Accessed: March 24, 2025, https://dace.unige.ch/opacityDatabase/?

Ehrenreich, D., Bourrier, V., Wheatley, P. J., et al. 2015, Nature, 522, 459, doi: 10.1038/nature14501

Ehrenreich, D., Lovis, C., Allart, R., et al. 2020, Nature, 580, 597, doi: 10.1038/s41586-020-2107-1

Einstein, A. 1936, Science, 84, 506, doi: 10.1126/science.84.2188.506

Espinoza, N., Rackham, B. V. \., Jordán, A., et al. 2019, Monthly Notices of the Royal Astronomical Society, 482, 2065, doi: 10.1093/mnras/sty2691

Farmer, C. B. 1966, Nature, 209, 1341, doi: 10.1038/2091341a0

Feinstein, A. D., Radica, M., Welbanks, L., et al. 2023, Nature, 614, 670, doi: 10.1038/s41586-022-05674-1

Finnerty, L., Xuan, J. W., Xin, Y., et al. 2024, The Astronomical Journal, 167, 43, doi: 10.3847/1538-3881/ad1180

Fletcher, L. N., Orton, G. S., Teanby, N. A., Irwin, P. G. J., & Bjoraker, G. L. 2009, Icarus, 199, 351, doi: 10.1016/j.icarus.2008.09.019

Fortney, J. J., Dawson, R. I., & Komacek, T. D. 2021, Journal of Geophysical Research (Planets), 126, doi: 10.1029/2020JE006629

Fortney, J. J., Lodders, K., Marley, M. S., & Freedman, R. S. 2008, The Astrophysical Journal, 678, 1419, doi: 10.1086/528370

Fortney, J. J., Saumon, D., Marley, M. S., Lodders, K., & Freedman, R. S. 2006, The Astrophysical Journal, 642, 495, doi: 10.1086/500920

Frommhold, L. 1994, Collision-induced Absorption in Gases, Cambridge Monographs on Atomic, Molecular and Chemical Physics (Cambridge: Cambridge University Press), doi: 10.1017/CBO9780511524523

Gandhi, S., Kesseli, A., Snellen, I., et al. 2022, Monthly Notices of the Royal Astronomical Society, 515, 749, doi: 10.1093/mnras/stac1744

Gandhi, S., Kesseli, A., Zhang, Y., et al. 2023, AJ, 165, 242, doi: 10.3847/1538-3881/accd65

Gandhi, S., de Regt, S., Snellen, I., et al. 2025, Monthly Notices of the Royal Astronomical Society, 537, 134, doi: 10.1093/mnras/staf004

Gaudi, B. S., & Winn, J. N. 2007, The Astrophysical Journal, 655, 550, doi: 10.1086/509910

Gaudi, B. S., Albrow, M. D., An, J., et al. 2002, The Astrophysical Journal, 566, 463, doi: 10.1086/337987

Gibson, N. P., Nugroho, S. K., Lothringer, J., Maguire, C., & Sing, D. K. 2022, Monthly Notices of the Royal Astronomical Society, 512, 4618, doi: 10.1093/mnras/stac091

Gibson, N. P., Merritt, S., Nugroho, S. K., et al. 2020, Monthly Notices of the Royal Astronomical Society, 493, 2215, doi: 10.1093/mnras/staa228

Gillon, M., Triaud, A. H. M. J., Demory, B.-O., et al. 2017, Nature, 542, 456, doi: 10.1038/nature21360

Gould, A., & Loeb, A. 1992, The Astrophysical Journal, 396, 104, doi: 10.1086/171700

Gould, A., Dong, S., Gaudi, B. S., et al. 2010, The Astrophysical Journal, 720, 1073, doi: 10.1088/0004-637X/720/2/1073

Gravity+ Collaboration, Abuter, R., Alarcon, P., et al. 2022, The Messenger, 189, 17, doi: 10.18727/0722-6691/5285

Grimm, S. L., & Heng, K. 2015, The Astrophysical Journal, 808, 182, doi: 10.1088/0004-637X/808/2/182

Grimm, S. L., Malik, M., Kitzmann, D., et al. 2021, The Astrophysical Journal Supplement Series, 253, 30, doi: 10.3847/1538-4365/abd773

Harada, C. K., Dressing, C. D., Kane, S. R., & Ardestani, B. A. 2024, The Astrophysical Journal Supplement Series, 272, 30, doi: 10.3847/1538-4365/ad3e81

Hatzes, A. P., Cochran, W. D., Endl, M., et al. 2003, The Astrophysical Journal, 599, 1383, doi: 10.1086/379281

Heger, M. L. 1919, Publications of the Astronomical Society of the Pacific, 31, 304, doi: 10.1086/122890

Helling, C., Lewis, D., Samra, D., et al. 2021, A&A, 649, A44, doi: 10.1051/0004-6361/202039911

Heng, K., & Marley, M. S. 2018, in Handbook of Exoplanets, ed. H. J. Deeg & J. A. Belmonte (Cham: Springer International Publishing), 2137–2152, doi: 10.1007/978-3-319-55333-7_102

Herman, M. K., de Mooij, E. J. W., Jayawardhana, R., & Brogi, M. 2020, The Astronomical Journal, 160, 93, doi: 10.3847/1538-3881/ab9e77

Hoeijmakers, H. J., de Kok, R. J., Snellen, I. A. G., et al. 2015, A&A, 575, A20, doi: 10.1051/0004-6361/201424794

Hoeijmakers, H. J., Ehrenreich, D., Heng, K., et al. 2018, Nature, 560, 453, doi: 10.1038/s41586-018-0401-y

Hoeijmakers, H. J., Ehrenreich, D., Kitzmann, D., et al. 2019, A&A, 627, A165, doi: 10.1051/0004-6361/201935089

Hoeijmakers, H. J., Seidel, J. V., Pino, L., et al. 2020, A&A, 641, A123, doi: 10.1051/0004-6361/202038365

Hoeijmakers, H. J., Kitzmann, D., Morris, B. M., et al. 2024, Astronomy and Astrophysics, 685, A139, doi: 10.1051/0004-6361/202244968

Holman, M. J., & Murray, N. W. 2005, Science, 307, 1288, doi: 10.1126/science.1107822

Holman, M. J., Fabrycky, D. C., Ragozzine, D., et al. 2010, Science, 330, 51, doi: 10.1126/science.1195778

Houllé, M., Vigan, A., Carlotti, A., et al. 2021, Astronomy & Astrophysics, 652, A67, doi: 10.1051/0004-6361/202140479

Hubbard, W. B., Fortney, J. J., Lunine, J. I., et al. 2001, The Astrophysical Journal, 560, 413, doi: 10.1086/322490

Hubeny, I., Burrows, A., & Sudarsky, D. 2003, The Astrophysical Journal, 594, 1011, doi: 10.1086/377080

Instituto de Astrofísica de Canarias. Accessed: February 5, 2025, ExoAtmospheres project, https://research.iac.es/proyecto/exoatmospheres/index.php

Johnson, S. A., Penny, M., Gaudi, B. S., et al. 2020, The Astronomical Journal, 160, 123, doi: 10.3847/1538-3881/aba75b

Kasper, M., Urra, N. C., Pathak, P., et al. 2021, Published in The Messenger vol. 182, pp. 38-43, 6 pages, doi: 10.18727/0722-6691/5221

Kasting, J. F. 1988, Icarus, 74, 472, doi: 10.1016/0019-1035(88)90116-9

Kausch, W., Noll, S., Smette, A., et al. 2015, Astronomy & Astrophysics, 576, A78, doi: 10.1051/0004-6361/201423909

Kitzmann, D., & Grimm, S. 2022, Astrophysics Source Code Library, ascl:2207.010

Kitzmann, D., Heng, K., Oreshenko, M., et al. 2020, The Astrophysical Journal, 890, 174, doi: 10.3847/1538-4357/ab6d71

Kitzmann, D., Heng, K., Rimmer, P. B., et al. 2018, ApJ, 863, 183, doi: 10.3847/1538-4357/aace5a

Komacek, T. D., & Showman, A. P. 2016, The Astrophysical Journal, 821, 16, doi: 10.3847/0004-637X/821/1/16

Kuiper, G. 1952, The atmospheres of the earth and planets (University of Chicago Press)

Langeveld, A. B., Deibert, E. K., Young, M. E., et al. 2025, The Astrophysical Journal Letters, 981, L32, doi: 10.3847/2041-8213/adb70d

Lecavelier Des Etangs, A., Ehrenreich, D., Vidal-Madjar, A., et al. 2010, Astronomy and Astrophysics, 514, A72, doi: 10.1051/0004-6361/200913347

Line, M. R., Wolf, A. S., Zhang, X., et al. 2013, The Astrophysical Journal, 775, 137, doi: 10.1088/0004-637X/775/2/137

Lothringer, J. D., Barman, T., & Koskinen, T. 2018, ApJ, 866, 27, doi: 10.3847/1538-4357/aadd9e

Lothringer, J. D., Rustamkulov, Z., Sing, D. K., et al. 2021, The Astrophysical Journal, 914, 12, doi: 10.3847/1538-4357/abf8a9

Lothringer, J. D., Bennett, K. A., Sing, D. K., et al. 2025, Refractory and Volatile Species in the UV-to-IR Transmission Spectrum of Ultra-hot Jupiter WASP-178b with HST and JWST, doi: 10.48550/arXiv.2503.15472

Lovis, C., & Fischer, D. 2010, Radial Velocity Techniques for Exoplanets (University of Arizona Press)

Lustig-Yaeger, J., Meadows, V. S., Crisp, D., Line, M. R., & Robinson, T. D. 2023, The Planetary Science Journal, 4, 170, doi: 10.3847/PSJ/acf3e5

Macintosh, B., Graham, J. R., Barman, T., et al. 2015, Science, 350, 64, doi: 10.1126/science.aac5891

Madhusudhan, N., Amin, M. A., & Kennedy, G. M. 2014, The Astrophysical Journal Letters, 794, L12, doi: 10.1088/2041-8205/794/1/L12

Madhusudhan, N., & Seager, S. 2009, The Astrophysical Journal, 707, 24, doi: 10.1088/0004-637X/707/1/24

Maguire, C., Gibson, N. P., Nugroho, S. K., et al. 2023, MNRAS, 519, 1030, doi: 10.1093/mnras/stac3388

Mao, S., & Paczynski, B. 1991, The Astrophysical Journal, 374, L37, doi: 10.1086/186066

Marconi, A., Abreu, M., Adibekyan, V., et al. 2024, in Ground-based and Airborne Instrumentation for Astronomy X, Vol. 13096 (SPIE), 478–503, doi: 10.1117/12.3017966

Marley, M. S., Ackerman, A. S., Cuzzi, J. N., & Kitzmann, D. 2013, Clouds and Hazes in Exoplanet Atmospheres, doi: 10.2458/azu_uapress_9780816530595-ch015

Marov, M. Y. 2004, Proceedings of the International Astronomical Union, 2004, 209, doi: 10.1017/S1743921305001390

Mayor, M., & Queloz, D. 1995, Nature, 378, 355, doi: 10.1038/378355a0

McKemmish, L. K., Masseron, T., Hoeijmakers, H. J., et al. 2019, MNRAS, 488, 2836, doi: 10.1093/mnras/stz1818

McLaughlin, D. B. 1924, The Astrophysical Journal, 60, 22, doi: 10.1086/142826

Merritt, S. R., Gibson, N. P., Nugroho, S. K., et al. 2021, MNRAS, 506, 3853, doi: 10.1093/mnras/stab1878

Mollière, P., Wardenier, J. P., van Boekel, R., et al. 2019, Astronomy & Astrophysics, 627, A67, doi: 10.1051/0004-6361/201935470

Narita, N., Suto, Y., Winn, J. N., et al. 2005, Publications of the Astronomical Society of Japan, 57, 471, doi: 10.1093/pasj/57.3.471

NASA Exoplanet Archive. Accessed: March 24, 2025, NASA Exoplanet Archive, https://exoplanetarchive.ipac.caltech.edu

Niemann, H. B., Atreya, S. K., Carignan, G. R., et al. 1998, Journal of Geophysical Research: Planets, 103, 22831, doi: 10.1029/98JE01050

Nortmann, L., Pallé, E., Salz, M., et al. 2018, Science, 362, 1388, doi: 10.1126/science.aat5348

Nortmann, L., Lesjak, F., Yan, F., et al. 2025, Astronomy & Astrophysics, 693, A213, doi: 10.1051/0004-6361/202450438

Nugroho, S. K., Kawahara, H., Masuda, K., et al. 2017, The Astronomical Journal, 154, 221, doi: 10.3847/1538-3881/aa9433

Palchetti, L., Bianchini, G., Carli, B., Cortesi, U., & Del Bianco, S. 2008, Atmospheric Chemistry and Physics, 8, 2885, doi: 10.5194/acp-8-2885-2008

Palle, E., Biazzo, K., Bolmont, E., et al. 2023, Ground-breaking Exoplanet Science with the ANDES spectrograph at the ELT, doi: 10.48550/arXiv.2311.17075

Parmentier, V., Guillot, T., Fortney, J. J., & Marley, M. S. 2015, Astronomy and Astrophysics, 574, A35, doi: 10.1051/0004-6361/201323127

Parmentier, V., Line, M. R., Bean, J. L., et al. 2018, Astronomy and Astrophysics, 617, A110, doi: 10.1051/0004-6361/201833059

Pelletier, S., Benneke, B., Ali-Dib, M., et al. 2023, Nature, doi: 10.1038/s41586-023-06134-0

Pelletier, S., Benneke, B., Chachan, Y., et al. 2024, The Astronomical Journal, 169, 10, doi: 10.3847/1538-3881/ad8b28

Penny, M. T., Gaudi, B. S., Kerins, E., et al. 2019, The Astrophysical Journal Supplement Series, 241, 3, doi: 10.3847/1538-4365/aafb69

Perryman, M., Hartman, J., Bakos, G. ⊠., & Lindegren, L. 2014, The Astrophysical Journal, 797, 14, doi: 10.1088/0004-637X/797/1/14

Picos, D. G., Snellen, I. a. G., Regt, S. d., et al. 2024, Astronomy & Astrophysics, 689, A212, doi: 10.1051/0004-6361/202450028

Pino, L., Ehrenreich, D., Wyttenbach, A., et al. 2018, Astronomy and Astrophysics, 612, A53, doi: 10.1051/0004-6361/201731244

Pino, L., Désert, J.-M., Brogi, M., et al. 2020, The Astrophysical Journal Letters, 894, L27, doi: 10.3847/2041-8213/ab8c44

Pino, L., Brogi, M., Désert, J. M., et al. 2022, Astronomy and Astrophysics, 668, A176, doi: 10.1051/0004-6361/202244593

Piskunov, N. E., Kupka, F., Ryabchikova, T. A., Weiss, W. W., & Jeffery, C. S. 1995, Astronomy and Astrophysics Supplement Series, 112, 525

Prinoth, B., Seidel, J. V., Hoeijmakers, H. J., et al. 2025, Astronomy & Astrophysics, 694, A284, doi: 10.1051/0004-6361/202452405

Rayleigh, L. 1899, XXXIV. On the transmission of light through an atmosphere containing small particles in suspension, and on the origin of the blue of the sky, Zenodo, doi: 10.1080/14786449908621276

Redfield, S., Endl, M., Cochran, W. D., & Koesterke, L. 2008, The Astrophysical Journal, 673, L87, doi: 10.1086/527475

Rossiter, R. A. 1924, The Astrophysical Journal, 60, 15, doi: 10.1086/142825

Rothman, L. S., Gordon, I. E., Babikov, Y., et al. 2013, Journal of Quantitative Spectroscopy and Radiative Transfer, 130, 4, doi: 10.1016/j.jqsrt.2013.07.002

Rustamkulov, Z., Sing, D. K., Mukherjee, S., et al. 2023, Nature, 614, 659, doi: 10.1038/s41586-022-05677-y

Saran, D. V., Slanger, T. G., Feng, W., & Plane, J. M. C. 2011, Journal of Geophysical Research: Atmospheres, 116, doi: 10.1029/2011JD015662

Seager, S., & Sasselov, D. D. 2000, The Astrophysical Journal, 537, 916, doi: 10.1086/309088

Sedaghati, E., Boffin, H. M. J., Jeřabková, T., et al. 2016, Astronomy & Astrophysics, 596, A47, doi: 10.1051/0004-6361/201629090

Sedaghati, E., Boffin, H. M. J., MacDonald, R. J., et al. 2017, Nature, 549, 238, doi: 10.1038/nature23651

Sedaghati, E., MacDonald, R. J., Casasayas-Barris, N., et al. 2021, MNRAS, 505, 435, doi: 10.1093/mnras/stab1164

Seidel, J. V., Ehrenreich, D., Pino, L., et al. 2020, Astronomy and Astrophysics, 633, A86, doi: 10.1051/0004-6361/201936892

Seidel, J. V., Ehrenreich, D., Wyttenbach, A., et al. 2019, Astronomy and Astrophysics, 623, A166, doi: 10.1051/0004-6361/201834776

Seidel, J. V., Ehrenreich, D., Allart, R., et al. 2021, A&A, 653, A73, doi: 10.1051/0004-6361/202140569

Seidel, J. V., Borsa, F., Pino, L., et al. 2023, A&A, 673, A125, doi: 10.1051/0004-6361/202245800

Seidel, J. V., Prinoth, B., Pino, L., et al. 2025, Nature, 1, doi: 10.1038/s41586-025-08664-1

Serindag, D. B., Nugroho, S. K., Mollière, P., et al. 2021, Astronomy & Astrophysics, 645, A90, doi: 10.1051/0004-6361/202039135

Silva, A. R. C., Demangeon, O. D. S., Santos, N. C., et al. 2024, Astronomy & Astrophysics, 689, A8, doi: 10.1051/0004-6361/202449935

Simkin, S. M. 1974, Astronomy and Astrophysics, 31, 129

Simonnin, A., Parmentier, V., Wardenier, J. P., et al. 2024, Time Resolved Absorption of Six Chemical Species With MAROON-X Points to Strong Drag in the Ultra Hot Jupiter TOI-1518 b, doi: 10.48550/arXiv.2412.01472

Sing, D. K., Désert, J. M., Fortney, J. J., et al. 2011, Astronomy and Astrophysics, 527, A73, doi: 10.1051/0004-6361/201015579

Smette, A., Sana, H., Noll, S., et al. 2015, Astronomy & Astrophysics, 576, A77, doi: 10.1051/0004-6361/201423932

Smith, P. C. B., Line, M. R., Bean, J. L., et al. 2024, The Astronomical Journal, 167, 110, doi: 10.3847/1538-3881/ad17bf

Snellen, I. A. G., Albrecht, S., de Mooij, E. J. W., & Le Poole, R. S. 2008, Astronomy & Astrophysics, 487, 357, doi: 10.1051/0004-6361:200809762

Snellen, I. A. G., Brandl, B. R., de Kok, R. J., et al. 2014, Nature, 509, 63, doi: 10.1038/nature13253

Snellen, I. A. G., de Kok, R. J., de Mooij, E. J. W., & Albrecht, S. 2010, Nature, 465, 1049, doi: 10.1038/nature09111

Sozzetti, A., Pinamonti, M., Damasso, M., et al. 2023, Astronomy & Astrophysics, 677, L15, doi: 10.1051/0004-6361/202347329

Spiegel, D. S., Silverio, K., & Burrows, A. 2009, ApJ, 699, 1487, doi: 10.1088/0004-637X/699/2/1487

Stefánsson, G., Mahadevan, S., Winn, J. N., et al. 2025, The Astronomical Journal, 169, 107, doi: 10.3847/1538-3881/ada9e1

Sun, H., Bouman, K. L., Tiede, P., et al. 2022, The Astrophysical Journal, 932, 99, doi: 10.3847/1538-4357/ac6be9

Symons, G. J. 1888, The eruption of krakatoa, and subsequent phenomena: report of the krakatoa committee of the royal society (Trübner & Company)

Tennyson, J., Yurchenko, S. N., Al-Refaie, A. F., et al. 2016, Journal of Molecular Spectroscopy, 327, 73

Tinetti, G., Drossart, P., Eccleston, P., et al. 2018, Experimental Astronomy, 46, 135, doi: 10.1007/s10686-018-9598-x

Tsapras, Y. 2018, Geosciences, 8, 365, doi: 10.3390/geosciences8100365

Visscher, C. 2022, in Oxford Research Encyclopedia of Planetary Science, doi: 10.1093/acrefore/9780190647926.013.17

von Fraunhofer, J. 1814, München, Königlichen Akademie der Wissenschaften, 5, 193

Wakeford, H. R., Sing, D. K., Deming, D., et al. 2018, The Astronomical Journal, 155, 29, doi: 10.3847/1538-3881/aa9e4e

Wardenier, J. P., Parmentier, V., Line, M. R., et al. 2024, Publications of the Astronomical Society of the Pacific, 136, 084403, doi: 10.1088/1538-3873/ad5c9f

Wishart, A. W. 1979, Monthly Notices of the Royal Astronomical Society, 187, 59P, doi: 10.1093/mnras/187.1.59P

Wolszczan, A., & Frail, D. A. 1992, Nature, 355, 145, doi: 10.1038/355145a0

Wright, J. T. 2018, Radial Velocities as an Exoplanet Discovery Method, doi: 10.1007/978-3-319-55333-7_4

Wright, J. T., & Gaudi, B. S. 2013, Exoplanet Detection Methods, doi: 10.1007/978-94-007-5606-9_10

Wyttenbach, A., Ehrenreich, D., Lovis, C., Udry, S., & Pepe, F. 2015, Astronomy & Astrophysics, 577, A62, doi: 10.1051/0004-6361/201525729

Wyttenbach, A., Mollière, P., Ehrenreich, D., et al. 2020, Astronomy & Astrophysics, 638, A87, doi: 10.1051/0004-6361/201937316

Yurchenko, S. N., & Tennyson, J. 2014, Monthly Notices of the Royal Astronomical Society, 440, 1649, doi: 10.1093/mnras/stu326

Zhang, Y., González Picos, D., de Regt, S., et al. 2024, The Astronomical Journal, 168, 246, doi: 10.3847/1538-3881/ad7ea9

Öberg, K. I., Murray-Clay, R., & Bergin, E. A. 2011, The Astrophysical Journal, 743, L16, doi: 10.1088/2041-8205/743/1/L16

Part II

Scientific Publications

Author contributions

A summary of my contribution to the papers included in this thesis.

Paper I

Titanium oxide and chemical inhomogeneity in the atmosphere of the exoplanet WASP-189 b

Prinoth, Bibiana; Hoeijmakers, H. Jens; Kitzmann, Daniel; Sandvik, Elin; Seidel, Julia V.; Lendl, Monika; Borsato, Nicholas W.; Thorsbro, Brian; Anderson, David R.; Barrado, David; Kravchenko, Kateryna; Allart, Romain; Bourrier, Vincent; Cegla, Heather M.; Ehrenreich, David; Fisher, Chloe; Lovis, Christophe; Guzmán-Mesa, Andrea; Grimm, Simon; Hooton, Matthew; Morris, Brett M.; Oreshenko, Maria; Pino, Lorenzo; Heng, Kevin

Nature Astronomy, Volume 6, p. 449-45 (2022)

In this study, I led the telluric correction, cross-correlation analysis, and post-processing of the detected species, including Doppler shadow correction, detrending of correlated noise and aliases, and model injection. I performed the fitting of the K_p–v_{sys} maps to obtain the best-fit parameters for the Gaussian models. The cross-correlation analysis was conducted with code developed by my supervisor, H. Jens Hoeijmakers, and used templates for single species and full atmospheric models computed by Daniel Kitzmann. I carried out the bootstrap analysis to test the robustness of candidate signals, and I co-led the writing of the manuscript.

Paper II

Time-resolved transmission spectroscopy of the ultra-hot Jupiter WASP-189 b

Prinoth, Bibiana; Hoeijmakers, H. Jens; Pelletier, Stefan; Kitzmann, Daniel; Morris, Brett M.; Seifahrt, Andreas; Kasper, David; Korhonen, Heidi H.; Burheim, Madeleine; Bean, Jacob L.; Benneke, Björn; Borsato, Nicholas W.; Brady, Madison; Grimm, Simon L.; Luque, Rafael; Stürmer, Julian; Thorsbro, Brian

Astronomy & Astrophysics, Volume 678, id.A182, 38 pp. (2023)

In this study, I led the data reduction of the newly obtained ESPRESSO transit (PI Prinoth), including telluric correction, cross-correlation analysis, and post-processing, following the same approach as in Paper I. I performed the time-resolved fits to the planetary trace and computed the ionisation curves and corresponding ionisation temperatures for the relevant species in the planet's atmosphere. I led the writing of the manuscript.

Paper III

An atlas of resolved spectral features in the transmission spectrum of WASP-189 b with MAROON-X

Prinoth, Bibiana; Hoeijmakers, H. Jens; Morris, Brett M.; Lam, Madeline; Kitzmann, Daniel; Sedaghati, Elyar; Seidel, Julia V.; Lee, Elspeth K. H.; Thorsbro, Brian; Borsato, Nicholas W.; Damasceno, Yuri C.; Pelletier, Stefan; Seifahrt, Andreas

Astronomy & Astrophysics, Volume 685, id.A60, 33 pp. (2024)

In this study, I led the telluric correction and narrow-band spectroscopy analysis, including corrections for sky emission and the Rossiter-McLaughlin effect. I developed and performed the retrieval routine for the joint fit of the Rossiter-McLaughlin effect and the planetary Ca^{+} absorption. The stellar model used in fitting the Rossiter-McLaughlin effect was computed by Madeline Lam. I led the writing of the manuscript.

Paper IV

High-resolution transmission spectroscopy of warm Jupiters: An ESPRESSO sample with predictions for ANDES

Prinoth, Bibiana; Sedaghati, Elyar; Seidel, Julia V.; Hoeijmakers, H. Jens; Brahm, Rafael; Thorsbro, Brian; Jordán, Andrés

The Astronomical Journal, Volume 168, Number 3 (2024)

In this study, I led the cross-correlation analysis using the code developed by my supervisor, H. Jens Hoeijmakers. I computed the cross-correlation templates and atmospheric models for the planets in the sample and performed injection-recovery tests for planetary signals observed with ESPRESSO and simulated for ANDES. I developed an observation simulator for ANDES and implemented support for eccentric orbits in my supervisor's code. Additionally, I developed a code to predict the velocity components of the planet, star, telluric contamination (for a given observation date), and the Rossiter-McLaughlin effect. I led the writing of the manuscript.

Printed by Media-Tryck, Lund 2025 NORDIC SWAN ECOLABEL 3041 0903

LUND UNIVERSITY

Faculty of Science
Department of Physics
Division of Astrophysics

ISBN 978-91-8104-360-0